Global Biogeochemical Cycles

RESEARCH ARTICLE
10.1029/2023GB007996

Significance of Urea in Sustaining Nitrite Production by Ammonia Oxidizers in the Oligotrophic Ocean

Xianhui S. Wan[1,2], Hua-Xia Sheng[2], Hui Shen[2], Wenbin Zou[2], Jin-Ming Tang[2], Wei Qin[3], Minhan Dai[2], Shuh-Ji Kao[2,4], and Bess B. Ward[1]

[1]Department of Geosciences, Princeton University, Princeton, NJ, USA, [2]State Key Laboratory of Marine Environmental Science, College of Ocean and Earth Sciences, Xiamen University, Xiamen, China, [3]School of Biological Sciences, Institute for Environmental Genomics, University of Oklahoma, Norman, OK, USA, [4]State Key Laboratory of Marine Resource Utilization in South China Sea, Hainan University, Haikou, China

Key Points:

- Active urea-derived nitrogen oxidation in the presence of added ammonium suggests direct urea utilization by marine ammonia oxidizers
- Substrate affinity regulates the vertical distribution of ammonia, urea, and nitrite in the ocean's interior
- Nitrite production from urea is comparable to that from ammonia oxidation in the energy-starved mesopelagic ocean

Supporting Information:

Supporting Information may be found in the online version of this article.

Correspondence to:

X. S. Wan,
xianhuiw@princeton.edu

Citation:

Wan, X. S., Sheng, H.-X., Shen, H., Zou, W., Tang, J.-M., Qin, W., et al. (2024). Significance of urea in sustaining nitrite production by ammonia oxidizers in the oligotrophic ocean. *Global Biogeochemical Cycles*, *38*, e2023GB007996. https://doi.org/10.1029/2023GB007996

Received 12 OCT 2023
Accepted 24 SEP 2024

Author Contributions:

Conceptualization: Xianhui S. Wan, Bess B. Ward
Data curation: Xianhui S. Wan, Minhan Dai, Shuh-Ji Kao, Bess B. Ward
Formal analysis: Xianhui S. Wan, Hua-Xia Sheng, Wei Qin, Bess B. Ward
Funding acquisition: Minhan Dai, Shuh-Ji Kao, Bess B. Ward
Investigation: Xianhui S. Wan, Hua-Xia Sheng, Hui Shen, Wenbin Zou, Jin-Ming Tang
Methodology: Xianhui S. Wan, Hua-Xia Sheng, Hui Shen, Wenbin Zou, Jin-Ming Tang
Resources: Minhan Dai, Shuh-Ji Kao, Bess B. Ward

Abstract Nitrification, the stepwise oxidation of ammonia to nitrate via nitrite, is a key process in the marine nitrogen cycle. Reported nitrite oxidation rates frequently exceed ammonia oxidation rates below the euphotic zone, raising the fundamental question of whether the two steps are balanced and if alternative sources contribute to nitrite production in the dark ocean. Here we present vertically resolved profiles of ammonia, urea, and nitrite oxidation rates and their kinetic traits in the oligotrophic Subtropical North Pacific. Our results show active urea-derived nitrogen oxidation (urea-N oxidation) in the presence of experimental ammonium amendment, suggesting direct urea utilization. The depth-integrated rates of urea-N oxidation and ammonia oxidation are comparable, demonstrating that urea-N oxidation is a significant source of nitrite. The additional nitrite from urea-N oxidation helps to balance the two steps of nitrification in our study region. Nitrifiers exhibit high affinity for their substrates, and the apparent half-saturation constants for ammonia and nitrite oxidation decrease with depth. The apparent half-saturation constant for urea-N oxidation is higher than that for ammonia oxidation and shows no clear vertical trend. Such kinetic traits may account for the relatively higher urea concentration than ammonium concentration in the ocean's interior. Moreover, a compilation of our results and reported data shows a trend of increased urea-N oxidation relative to ammonia oxidation from the eutrophic coastal zone to the oligotrophic open ocean. This trend reveals a substrate-dependent biogeographic distribution of urea-N oxidation across marine environments and provides new information on the balance and flux of the marine nitrification process.

1. Introduction

Nitrification is a key process of the nitrogen cycle, linking the source and sink of fixed nitrogen, regulating the bioavailability of nitrogen, and contributing to nitrous oxide production and oxygen consumption. In the marine environment, nitrification consists of two steps: the oxidation of ammonia and ammonium (NH_3 and NH_4^+, hereafter referred to as NH_4^+) to nitrite (NO_2^-) by ammonia-oxidizing archaea and bacteria (AOA and AOB), and the oxidation of NO_2^- to nitrate (NO_3^-) by nitrite-oxidizing bacteria (NOB). Ammonia oxidation is generally assumed to be the rate-limiting step owing to the absence of NO_2^- accumulation in the global ocean, with a few exceptions such as the base of the euphotic zone, the oxygen-deficient zone, some eutrophied waters, and throughout the mixed layer the polar oceans (Casciotti, 2016; Wan et al., 2021; Ward, 2008; Zakem et al., 2018). This idea is supported by recent measurements showing that the rate of nitrite oxidation outpaces ammonia oxidation below the euphotic zone of the global ocean, despite the significantly higher abundance of AOA than NOB (Santoro et al., 2019; W. Tang et al., 2023). These observations, however, raise a fundamental question of whether alternative nitrogen sources are required to maintain the high AOA population and sustain the balance of the two nitrification steps in the vast dark ocean.

Urea, which is produced from multiple sources, including organic decomposition, viral lysis, phytoplankton and zooplankton excretion, and anthropogenic discharges, is a key DON component in the marine environment (Sipler & Bronk, 2015). Mounting evidence from culture and field studies suggests that many AOA and AOB are able to utilize urea, suggesting a potentially critical role for urea in sustaining the energy metabolism of ammonia oxidizers (Bayer et al., 2016; Carini et al., 2018; Kitzinger et al., 2019; Qin et al., 2024). Notably, urea concentration appears to be higher than NH_4^+ concentration in a variety of open ocean systems, for example, the euphotic and mesopelagic zone in the Arctic Ocean (Alonso-Sáez et al., 2012; Shiozaki et al., 2021); the euphotic zone in the Northwestern Pacific (NWP) (Wan et al., 2021); the upper 300 m in the Eastern Tropical North Pacific

Validation: Xianhui S. Wan, Hua-Xia Sheng, Wei Qin, Minhan Dai, Shuh-Ji Kao, Bess B. Ward
Visualization: Xianhui S. Wan, Hua-Xia Sheng
Writing – original draft: Xianhui S. Wan, Bess B. Ward
Writing – review & editing: Xianhui S. Wan, Hua-Xia Sheng, Hui Shen, Wenbin Zou, Jin-Ming Tang, Wei Qin, Minhan Dai, Shuh-Ji Kao, Bess B. Ward

(Widner et al., 2018); and the full water column in the South China Sea (SCS) (Chen et al., 2015). However, quantitative comparisons between urea-derived nitrogen oxidation (hereafter referred to as urea-N oxidation) and ammonia oxidation in the ocean remain sparse. The limited available data show that the relationship between the rates of urea-N and ammonia oxidation is highly variable in both coastal areas (Damashek et al., 2019; Kitzinger et al., 2019; J. M. Tang et al., 2022; W. Tang et al., 2022) and open ocean systems (Laperriere et al., 2021; Shiozaki et al., 2021; Tolar et al., 2017; Xu et al., 2019), and the underlying reason is still poorly understood.

Another unresolved key issue is whether urea-N oxidation occurs directly (i.e., urea is taken up, hydrolyzed, and oxidized by ammonia oxidizers) or indirectly (i.e., urea decomposition by other microbes provides NH_4^+ for oxidation by the ammonia oxidizers), or both, in the ocean. Although urea utilization by AOA and AOB has been recently studied in various marine systems using different approaches (e.g., ^{14}C labeling incubation, ^{15}N labeling incubation, biomarker genes and their transcription analysis, etc.), there is little consensus in the current literature (e.g., Alonso-Sáez et al., 2012; Kitzinger et al., 2019; Santoro et al., 2017; Smith et al., 2016; Tolar et al., 2017). For instance, in the Arctic Ocean and the Central Equatorial Pacific, the significant correlation between archaeal *amoA* and *ureC* gene abundance is interpreted as evidence for potential direct urea-N oxidation by marine AOA (Alonso-Sáez et al., 2012; Santoro et al., 2017). However, that conclusion is not supported by gene expression data showing no transcription of *ureC* in the Northeast Pacific (Smith et al., 2016). In the shelf region of the Gulf of Mexico, direct urea-N oxidation contributes to over half of the observed urea-N oxidation rate, although the urea-N oxidation rate accounts for only ~7% of the ammonia oxidation rate (Kitzinger et al., 2019). In addition to the inconsistencies reported in prior studies, the fractions of direct and indirect urea-N oxidation, and how the urea-N oxidation rate responds to the addition of NH_4^+ are still unclear. The contribution of urea-N oxidation to NO_2^- production appears to be more important in the oligotrophic open ocean than in the coastal waters (Tolar et al., 2017). Information on urea-N oxidation in the oligotrophic ocean thus holds the key to better understanding the balance of the two steps of nitrification in the ocean and the source of NO_2^-, which is a key intermediate in the marine nitrogen cycle (Casciotti, 2016).

The kinetic properties of nitrifiers in utilizing their substrates are considered as the primary determinant of their competitiveness and ecological niche (Jung et al., 2022; Martens-Habbena et al., 2009). Mounting evidence shows that marine ammonia and nitrite oxidizer natural populations have extremely high affinity (i.e., the measured apparent half saturation constant, hereafter referred as K_s, is at nanomolar level) for NH_4^+ and NO_2^- in the open ocean (e.g., L. Liu et al., 2023; Peng et al., 2016; Sun et al., 2017; Wan et al., 2018), demonstrating their ability to access substrates at the trace levels at which they occur in the ocean. The kinetic characterization of the ureolytic marine AOA species *Nitrosopumilus piranensis* indicates its higher affinity for NH_4^+ than for urea (Qin et al., 2024). The only available field study on the K_s of urea-N oxidation reported a range of 146–700 nmol N L^{-1} in the upper euphotic zone of the NWP (Xu et al., 2019). However, there is currently no information available on the kinetics of urea-N oxidation rate in the mesopelagic ocean, resulting in a knowledge gap about the affinity and energy generation strategy of marine nitrifiers in the NH_4^+-starved dark ocean. Quantifying and comparing the K_s of ammonia, urea, and nitrite oxidation thus holds the key to enhancing our understanding of marine nitrification homeostatic balance and the distribution of NH_4^+, urea, and NO_2^- in the global ocean.

The subtropical gyres cover nearly 30% of the global ocean surface and are characterized by permanent stratification and oligotrophic conditions. These vast ecosystems play an important role in marine biogeochemistry and are expected to further expand under global warming (Dai et al., 2023; Irwin & Oliver, 2009; Polovina et al., 2008). Despite the extremely low primary productivity and NH_4^+ supply, AOA comprise a major fraction of total prokaryotes below the euphotic zone in the oligotrophic gyres (Karner et al., 2001; Santoro et al., 2019), suggesting alternative substrates for AOA. We hypothesize that urea might play an important role in sustaining the energy generation of AOA to maintain their high abundance in the oligotrophic subtropical gyres, especially in the dark ocean where NH_4^+ supply is more limited than in the euphotic zone. To address these critical knowledge gaps, we investigated the distribution of ammonia, urea, and nitrite oxidation rates extending from the coastal zone of China into the SCS and the western North Pacific Subtropical Gyre (wNPSG). Using the results measured in our study, and by compiling the published data on urea-N oxidation rates reported in the global ocean, the primary motivations of our study are to: (a) measure the rates and determine kinetic traits of ammonia, urea, and nitrite oxidation across large substrate concentration and productivity gradients; (b) characterize the importance of urea-N oxidation to NO_2^- production; and (c) elucidate the spatial distribution of urea and ammonia oxidation in the global ocean.

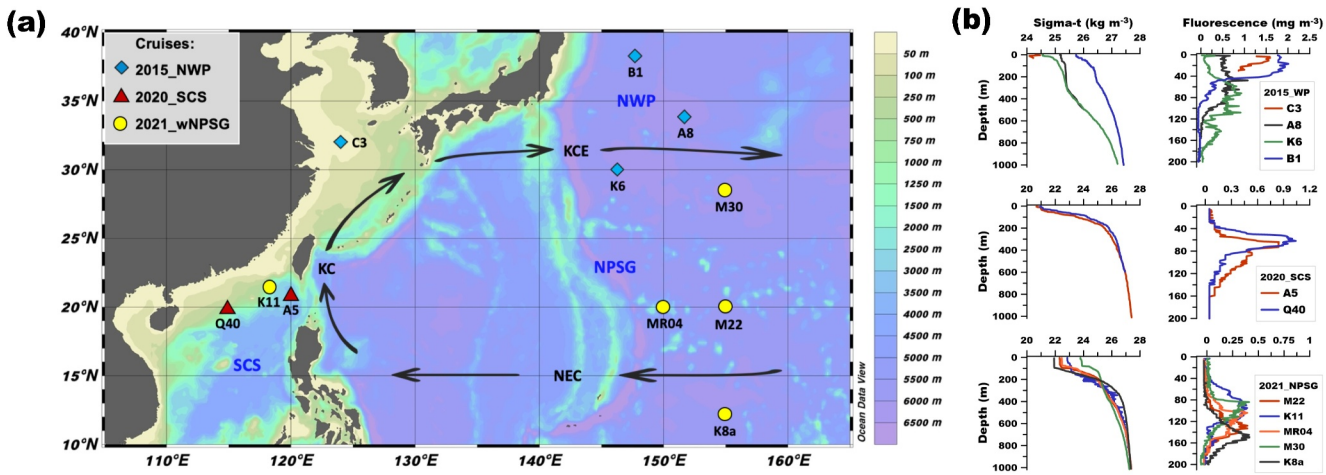

Figure 1. Study area and physical properties of the sampling stations. (a) Research area and sampling stations. Diamonds, triangles and dots show stations during the 2015 NWP, 2020 SCS, and 2021 wNPSG cruises, respectively. The black arrows denote the main surface currents of the NPSG. NEC, KC, and KCE are abbreviations of the North Equatorial Current, Kuroshio Current, and Kuroshio Current Extension, respectively. (b) Potential density anomaly and fluorescence profiles of the sampling stations during each cruise.

2. Materials and Methods

2.1. Sample Collection and On-Deck Incubations

Samples were collected from three research cruises conducted during 2015–2021 to the NWP (aboard R/V *Dongfanghong II*), the SCS, and the wNPSG (aboard R/V *Tan Kah Kee*). A total of 11 stations extending from the coastal shelf to the open ocean were investigated (Figure 1a; Table S1 in Supporting Information S1). On each cruise, temperature, salinity, depth and fluorescence were measured using a Seabird SBE 911 CTD sensor package equipped with a fluorometer sensor. Discrete seawater samples were collected using 24 12-L Niskin bottles mounted on the CTD rosette. We focus on the upper 1,000 m (the lower boundary of the mesopelagic ocean), as the rates at greater depths are too low to be detected using the isotope labeling incubation.

Samples for chemical, biological and rate measurements were collected from the same cast. Three 125 mL high-density polyethylene (HDPE) bottles (Nalgene, USA) or 50 mL centrifuge tubes (Fisher Scientific, USA) were used for nutrient collection. Samples for analysis of urea concentrations were collected into acid-washed, pre-combusted (450°C for 4 hr) 50 mL amber glass vials. Seawater for isotope labeling incubation was subsampled into 250 mL HDPE bottles. All bottles and equipment were acid-washed and rinsed with in situ seawater at least three times prior to sample collection. Onboard incubations were conducted at four stations across the shelf to the open ocean of the NWP, at three of the stations in the SCS slope and basin and four stations in the wNPSG. Multiple isotope labeling experiments were carried out to quantify the ammonia, urea-N and nitrite oxidation rates. Substrate kinetics for each process were determined at eight selected stations (Table S1 in Supporting Information S1). On the 2015 cruise to the NWP, an additional ^{15}N-L-Glutamic acid (^{15}N-Glu) labeling incubation was performed to compare the oxidation of urea versus glutamic acid.

For the profile rates of ammonia and urea-N oxidation, 1 mL of $^{15}N\text{-}NH_4^+$ or ^{15}N-Urea (99% of ^{15}N atom, Cambridge Isotope) and 0.5 mL of $^{14}N\text{-}NO_2^-$ carrier were added to each HDPE incubation bottle with 250 mL seawater to get a final tracer concentration of 20 nmol N L^{-1} and $^{14}N\text{-}NO_2^-$ carrier concentration of 0.5 µmol N L^{-1}. For profile NO_2^- oxidation rates, 1 mL of $^{15}N\text{-}NO_2^-$ (99% of ^{15}N atom, Cambridge Isotope) was added to incubation bottles to get a final concentration of 20 nmol N L^{-1}. For the kinetics experiments, samples from selected depths and stations were incubated at five to six different levels of tracer addition spanning from 10 to 1,000 nmol L^{-1} (Table S1 in Supporting Information S1). To test whether the measured urea-N oxidation was direct or indirect, an additional experiment was carried out on the NWP cruise. Specifically, the water samples were amended with four tracer treatments: 100 nmol N L^{-1} of ^{15}N-Urea; 100 nmol N L^{-1} of ^{15}N-Glu (98% of ^{15}N atom, Sigma-Aldrich); 100 nmol N L^{-1} of ^{15}N-Urea plus 2,000 nmol N L^{-1} of $^{14}NH_4^+$; and 100 nmol N L^{-1} of ^{15}N-Glu plus 2,000 nmol N L^{-1} of $^{14}NH_4^+$. The experiment with unlabeled NH_4^+ enrichment was designed to examine whether the $^{15}NO_2^-$ was produced via direct or indirect oxidation of ^{15}N labeled substrates: If the

$^{15}NH_4^+$ from the ^{15}N-urea or ^{15}N-Glu was produced via heterotrophic degradation, then the $^{15}NO_2^-$ production rate should decrease substantially in the presence of added $^{14}NH_4^+$ (a reduction by 95% because the tracer concentration only accounts for 5% of unlabeled NH_4^+ pool). Otherwise, if the labeled urea or glutamic acid was taken up by AOA, then the decrease in production of $^{15}NO_2^-$ should be less than the predicted 95% decrease. Incubations were performed at three time points (0, 12, and 24 hr). Immediately after injection of tracer and carrier, ~40 mL of sample was filtered through a 0.2 μm syringe filter to preserve for analysis of initial conditions. The remaining samples were kept in a series of temperature-controlled incubators close to in situ temperature (±2°C) in the dark for 12 and 24 hr and were terminated by filtration through 0.2 μm syringe filters. Filtered samples were stored at −20°C after collection. All incubations were implemented in triplicate.

2.2. Sample Analysis

NH_4^+ concentrations were measured aboard the research vessel immediately after collection using a fluorometric method with a detection limit of 1.2 nmol N L^{-1} and precision of ±3.5% (Zhu et al., 2013). Seawater samples for quantifying concentrations of other nutrients were stored at −20°C until measurements in the shore-based lab. Urea concentrations were measured using a liquid waveguide capillary cell based on the colorimetric reaction with diacetyl monoxime with a detection limit of 1 nmol N L^{-1} (Chen et al., 2015). NO_2^- and NO_3^- below the nitracline were measured using a four-channel Continuous Flow Technicon AA3 Auto-Analyzer (Bran-Lube, GmbH), with detection limits of 40 and 70 nmol N L^{-1}, respectively, and precision better than 1% (determined by repeated measurements of aged deep seawater at 10-sample intervals). Samples with concentrations of NO_3^- and NO_2^- that were near or below the detection limit of the AA3 were analyzed using standard colorimetric methods coupled to a Flow Injection Analysis-Liquid Waveguide Capillary Cell system (World Precision Instruments) with a lower detection limit of 5 nmol N L^{-1} and precision of better than 3% (J. Z. Zhang, 2000).

$\delta^{15}N$ of NO_2^- was measured by chemical conversion (sodium azide, Sigma-Aldrich) of NO_2^- to N_2O (Mcllvin & Altabet, 2005). To determine NO_2^- oxidation rates, the residual NO_2^- was removed from samples by adding sulfamic acid (≥99% sulfamic acid, Sigma-Aldrich) (Granger & Sigman, 2009) and the $\delta^{15}N$ of NO_3^- was determined using the bacterial denitrifier method (Weigand et al., 2016) with minor modifications. Briefly, NO_3^- was quantitatively converted to N_2O using the bacterial strain *Pseudomonas aureofaciens* (ATCC No. 13985), and N_2O was quantified using a Thermo Finnigan Gasbench system (including cryogenic extraction and purification) interfaced to a Delta V^{PLUS} isotopic ratio mass spectrometer (IRMS). $\delta^{15}N$ of NO_2^- values were calibrated against three in-house NO_2^- standards ($\delta^{15}N$ of the three in-house NO_2^- standards were determined using the bacterial method, with values of 0.5 ± 0.4‰, 22.1 ± 0.5‰, and 96.3 ± 0.6‰, respectively). Standard curves were run at the beginning and end of sample analysis and at 10 sample intervals to monitor any instrumental drift and memory effect during the sample measurement. Precision (pooled standard deviation) based on analyses of standards at 10 nmol N was ±0.4‰. $\delta^{15}N$ of NO_3^- values were calibrated against NO_3^- isotope standards USGS 34, IAEA N3, and USGS 32, which were run before, after, and at 10 sample intervals. Precision (pooled standard deviation) was better than ±0.3‰ according to analyses of these standards at an injection level of 10 nmol N. For samples with NO_3^- concentrations lower than 0.5 μmol N L^{-1}, 1 mL of 5 μmol N L^{-1} of in-house NO_3^- standard was added as carrier to 9 mL of seawater sample, and the isotopic composition of the sample was then calculated from the measured composition of the mixture and the known in-house standard via mass conservation. The propagated standard deviation was 0.42‰ for these samples (Wan et al., 2018).

2.3. Rate Calculation

The reaction rates were determined based on the accumulation of ^{15}N in the product pool relative to the initial (time zero) conditions. To minimize the potential enhancement of the in situ rates due to enrichment by tracer concentrations, the final concentrations of ^{15}N-NH_4^+, ^{15}N-urea and ^{15}N-NO_2^- were limited to 20 nmol L^{-1}. The final concentrations of NH_4^+, urea and NO_2^- in our incubations were close to or lower than the K_s measured in our study and the reported values for ammonia oxidation, urea-N oxidation and nitrite oxidation rates measured in the wNPSG and the NWP (L. Liu et al., 2023; Xu et al., 2019), suggesting an overall substrate limiting condition in our incubations. Therefore, we applied a linear regression approach using Equations 1 and 2 to obtain the estimates of the in situ reaction rates (Wan et al., 2018).

$$R_{\text{bulk}} = \frac{C_t \times n_t - C_0 \times n_0}{t \times f^{15}} \times 24 \quad (1)$$

$$R_{in\ situ} = R_{\text{bulk}} \times \frac{Ci_s}{Ci_s + Ct_s} \quad (2)$$

R_{bulk} is the bulk reaction rate for all substrates after tracer enrichment (nmol N L^{-1} d^{-1}); Ct and C_0 is the product concentration at the ending and beginning of the incubation (nmol N L^{-1}); f^{15} is at% ^{15}N of the substrate pool at the beginning of the incubation; n_t and n_0 are the at% ^{15}N of the product pool at the ending and beginning of the incubation (%), respectively; t is the duration of the incubation (h); $R_{in\ situ}$ is the in situ reaction rate calibrated by linear interpolation; and Ci_s and Ct_s are the initial substrate concentration and final tracer concentration, respectively. $R_{in\ situ}$ data are the results reported and discussed below. Notably, not all the kinetic tests show a typical Michaelis-Menten (M-M) type response. Lack of M-M type response has been attributed to trace metal nutrient limitation (Horak et al., 2013) or substrate saturation (Mdutyana, Sun, et al., 2022), resulting in uncertainty in using kinetic parameters to calibrate the substrate tracer enrichment effect. Nevertheless, given the general substrate limitation and the low tracer concentration (20 nmol N L^{-1}) used here, this method still represents a reliable and widely used approach for deriving the in situ rates in substrate-limited environments.

The depth-integrated (0–1,000 m) rate was derived using trapezoidal extrapolation of the in situ reaction rate.

The kinetic response of each process was quantified using the M-M Equation 3.

$$R_i = \frac{V_{\max} \times Ci_s}{K_s + Ci_s} \quad (3)$$

R_i is the reaction rate for all substrates after tracer enrichment (nmol N L^{-1} d^{-1}); $V_{\max}$ is the potential maximum rate (nmol N L^{-1} d^{-1}); K_s is the half saturation constant (nmol N L^{-1}); Ci_s is the bulk substrate concentration (i.e., in situ concentration plus tracer addition; nmol N L^{-1}). $V_{\max}$ and K_s were derived based on fitting the curve of the M-M function (Equation 3) using the measured rates and the substrate concentrations. The error of the kinetic parameters was determined as the standard error of the regression coefficient.

2.4. Detection Limits and Statistical Analysis

The detection limits of ammonia, urea-N and nitrite oxidation rates depend on the concentration of the product pool and the fraction of ^{15}N in the substrate pool during the incubation. The precision of $\delta^{15}N\text{-}NO_3^-$ and $\delta^{15}N\text{-}NO_2^-$ isotope composition measurements was better than ±0.3‰ and ±0.4‰ respectively, and here, we used 3 times the standard deviation as a minimum enrichment of ^{15}N in each product pool. Therefore, we calculated detection limits of 0.01–0.05, 0.01–0.10, and 0.01–0.90 nmol N L^{-1} d^{-1} for ammonia oxidation, urea-N oxidation, and nitrite oxidation, respectively. The comparisons of substrate concentrations, reaction rates and kinetic parameters were examined using the Mann-Whitney U-test. A p-value of <0.05 was considered significant.

2.5. Compilation of Ammonia Oxidation and Urea-N Oxidation Rates Measured in the Ocean

To investigate the spatial pattern of urea-N oxidation and ammonia oxidation rates and examine the potential environmental controls on the relationship between urea and ammonia oxidation rates, we compiled the available published data for simultaneous marine urea and ammonia oxidation rate measurements. Specifically, we collected NH_4^+ and urea concentrations, and ammonia and urea-N oxidation rates when both the concentrations and rates were measured simultaneously. To ensure accurate quantitative rate comparison and rate ratio calculation, rates which were reported as below the detection limits in the original literature were not included in the compilation. A total of 175 measurements were collected for analysis from study areas extending from the coastal ocean (i.e., estuaries, shelf, bottom depth < 200 m), including the Gulf of Mexico, the Chesapeake Bay, the Coast of Georgia in the US, the East China Sea, the Jiulong River Estuary in China, and the coast of Arctic Ocean (Damashek et al., 2019; Kitzinger et al., 2019; Shiozaki et al., 2021; J. M. Tang et al., 2022; W. Tang et al., 2022; Tolar et al., 2017; Xu et al., 2019), to the slope and open ocean systems (bottom depth > 200 m) including the NPSG, the NWP, the Southern Ocean, the South Atlantic Bight, the slope of Arctic Ocean and the Gulf of Alaska (Damashek et al., 2019; Shiozaki et al., 2021; Tolar et al., 2017; Wan et al., 2021; Xu et al., 2019), and the data measured in the SCS and the wNPSG in this study. Moreover, because different ammonia-oxidizing lineages show distinct NH_4^+ and urea preferences (Qin et al., 2024), and taking into account the fundamental control of

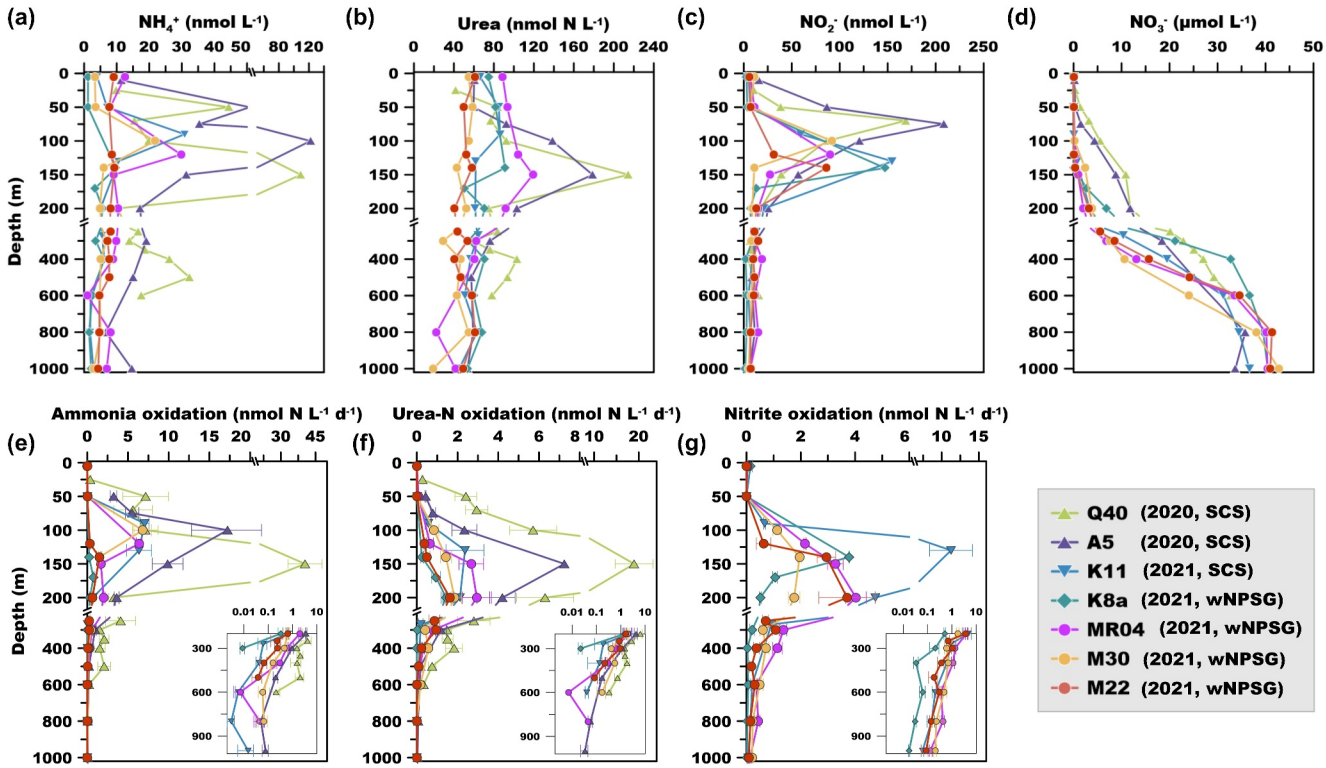

Figure 2. Nitrogen nutrient distribution and nitrification rate profiles. (a–d) Depth profiles of NH_4^+, Urea, NO_2^-, and NO_3^- in the SCS (2020 cruise) and the wNPSG (2021 cruise) stations, respectively. (e–g) In situ rates of ammonia oxidation, urea-N oxidation and nitrite oxidation, respectively. The error bars denote one standard deviation of triplicate rate measurements; in some cases, the error bars are smaller than the symbols. The insert panels depict the rate in the mesopelagic zone. Note that the concentrations and rates are shown in different scales, and the rates in the insert panels are shown in log scale.

substrate concentration on nitrifier community structure and activity (e.g., Martens-Habbena et al., 2009; Santoro et al., 2019), we grouped the collected data into three categories: the eutrophic coastal waters; the epipelagic zone (surface to 200 m) in the slope and open ocean where the AOA community is dominated by the Water Column A ecotype; and the mesopelagic zone (200–1,000 m) where the AOA community is dominated by the Water Column B ecotype (Francis et al., 2005; Qin et al., 2020; Santoro et al., 2019).

3. Results

3.1. Hydrography and Nitrogen Nutrient Distributions

The T-S diagram, the potential density anomaly, and fluorescence profiles showed distinct physical properties of the three study areas (Figure 1b; Figure S1 in Supporting Information S1). The density gradient was highest in the epipelagic layer of the SCS, but was less pronounced in the mesopelagic zone of the SCS compared to the wNPSG due to more intense vertical mixing at the basin scale in the SCS (Zhu et al., 2019). The NWP stations were characterized by the lowest density gradient. The deep chlorophyll maximum (DCM), as indicated by the fluorescence, showed a northward shoaling from the subtropical gyre to the higher latitude, accompanied by an increased chlorophyll maximum concentration, implying a northward intensification of biomass and primary productivity (Table S2 in Supporting Information S1).

NH_4^+ concentrations were consistently low (i.e., <20 nmol L^{-1}) at the SCS and the wNPSG stations with a few exceptions of maxima (e.g., ~100 nmol L^{-1}) at the base of the euphotic zone of the SCS stations (Figure 2a). The depth-integrated NH_4^+ inventory (0–1,000 m) ranged from 3.5 to 8.3 mmol N m^{-2} in the wNPSG, and was 5.2–20.1 mmol N m^{-2} in the SCS (Table 1). Urea concentrations showed no clear vertical pattern with two exceptions at the base of the euphotic zone at stations Q40 and A5 in the SCS (Figure 2b). The urea concentration (1–119 nmol N L^{-1}, median 51.6 nmol N L^{-1}) was significantly higher than NH_4^+ concentration (1–109 nmol L^{-1}, median 8.0 nmol L^{-1}) ($p < 0.01$). The depth integrated urea inventory was 44.5–66.1 mmol N m^{-2} in the wNPSG,

Table 1
Depth-Integrated (0–1,000 m) Inventory of Nitrogen Nutrient and Rates of the Three Measured Processes

	Q40	A5	K11	K8a	MR04	M30	M22
Water column inventory (0–1,000 m, mmol N m^{-2} for NH_4^+, Urea and NO_2^-; mol m^{-2} for NO_3^-)							
NH_4^+	17.0	20.1	5.2	3.5	8.3	5.6	6.5
Urea	55.4	73.9	59.6	66.1	57.2	44.5	49.4
NO_2^-	15.2	25.2	18.3	12.5	17.8	11.7	13.6
NO_3^-	15.4	29.5	28.2	34.8	29.5	27.4	41.3
Depth-integrated rate (0–1,000 m, mmol N m^{-2} d^{-1})							
Ammonia oxidation	3.50 ± 0.29	1.87 ± 0.14	0.70 ± 0.06	0.06 ± 0.01	0.65 ± 0.02	0.53 ± 0.04	0.15 ± 0.01
Urea oxidation	2.15 ± 0.17	1.03 ± 0.06	0.35 ± 0.06	0.14 ± 0.01	0.49 ± 0.05	0.42 ± 0.03	0.27 ± 0.02
Nitrite oxidation	ND	ND	1.25 ± 0.15	0.34 ± 0.01	1.02 ± 0.03	0.62 ± 0.03	0.60 ± 0.05

Note. ND: nitrite oxidation rate was not measured at stations Q40 and A5.

and was 55.9–73.9 mmol N m^{-2} in the SCS. Therefore, the urea inventory was 3.3–11.5-fold greater than the NH_4^+ inventory in the SCS, and the ratio increased to 6.6–18.9 in the wNPSG, suggesting an elevated stock of urea relative to NH_4^+ in the more oligotrophic region.

Prominent primary NO_2^- maxima (PNM) were detected at all the SCS and the wNPSG stations (Figure 2c). The depth of the NO_2^- maximum was deeper (100–140 m) and maximum concentration (86–147 nmol L^{-1}) was lower in the wNPSG compared to the SCS (i.e., depth ranged from 70 to 130 m, concentration ranged from 155 to 208 nmol L^{-1}), resulting in a higher depth-integrated NO_2^- inventory (0–1,000 m) in the SCS (15.2–25.2 mmol N m^{-2}) compared to the wNPSG (11.7–17.8 mmol N m^{-2}). NO_3^- concentrations remained low in the upper mixed layer at all stations (i.e., <1 μmol L^{-1}), and the depth of the nitracline (here defined as the first depth with NO_3^- concentration >1 μmol L^{-1} (Shiozaki et al., 2011)) was shallower in the SCS than in the wNPSG (Figure 2d). The depth-integrated NO_3^- inventory was higher in the wNPSG (27.4–43.1 mol N m^{-2}) than in the SCS (15.4–29.5 mol N m^{-2}) (Table 1). In the NWP cruise stations, the vertical sampling resolution was lower than that in the SCS and wNPSG stations, and the measured nitrogen nutrient concentrations in the NWP stations (Table S3 in Supporting Information S1) were higher than the SCS and wNPSG stations.

3.2. Ammonia, Urea, and Nitrite Oxidation Rate Profiles

Ammonia and urea-N oxidation rate depth profiles (0–1,000 m) were measured at seven stations in the SCS and the wNPSG, and the nitrite oxidation rate was quantified at five stations in the wNPSG. All the profiles demonstrated a similar vertical pattern with a prominent subsurface rate maximum (Figures 2e–2g). The rates were consistently low to undetectable in the upper mixed layer where nutrients were depleted at all stations, and increased rapidly to the depth of maximum rate (Figure 2). Ammonia and urea-N oxidation rates peaked at shallower depths (90–170 m) compared to the depth of the highest nitrite oxidation rate (130–200 m, Table S2 in Supporting Information S1). In the epipelagic layer, the ammonia oxidation rate ranged from below the detection limit to 40.5 nmol N L^{-1} d^{-1} (median 1.7 nmol N L^{-1} d^{-1}) and the urea-N oxidation rate ranged from below the detection limit to 19.0 nmol N L^{-1} d^{-1} (median 1.5 nmol N L^{-1} d^{-1}). In the mesopelagic layer, ammonia oxidation ranged from below the detection limit to 4.1 nmol N L^{-1} d^{-1} (median 0.1 nmol N L^{-1} d^{-1}); and urea-N oxidation ranged from below the detection limit to 2.8 nmol N L^{-1} d^{-1} (median 0.3 nmol N L^{-1} d^{-1}) (Figures 2e and 2f, inserted panels). Although the peak ammonia oxidation rate was higher than that of the urea-N oxidation rate, the two rates were not statistically different ($p > 0.05$). The nitrite oxidation rate (ranged from below the detection limit to 11.3 nmol N L^{-1} d^{-1}, median 0.4 nmol N L^{-1} d^{-1}) was higher than the ammonia oxidation rate ($p < 0.01$) and urea-N oxidation rate ($p < 0.05$) (Figure 2g).

The depth-integrated (0–1,000 m) urea-N oxidation rate accounted for 34%–71% (median 43%) of the total nitrite production from ammonia and urea, suggesting a substantial contribution of urea-N oxidation to NO_2^- production in the oligotrophic ocean (Table 1). The integrated rates were positively correlated with primary productivity ($p = 0.007$ for ammonia oxidation and 0.016 for urea oxidation; inferred from the depth-integrated fluorescence, Figure S2 in Supporting Information S1), because primary production determines the light attenuation, and the

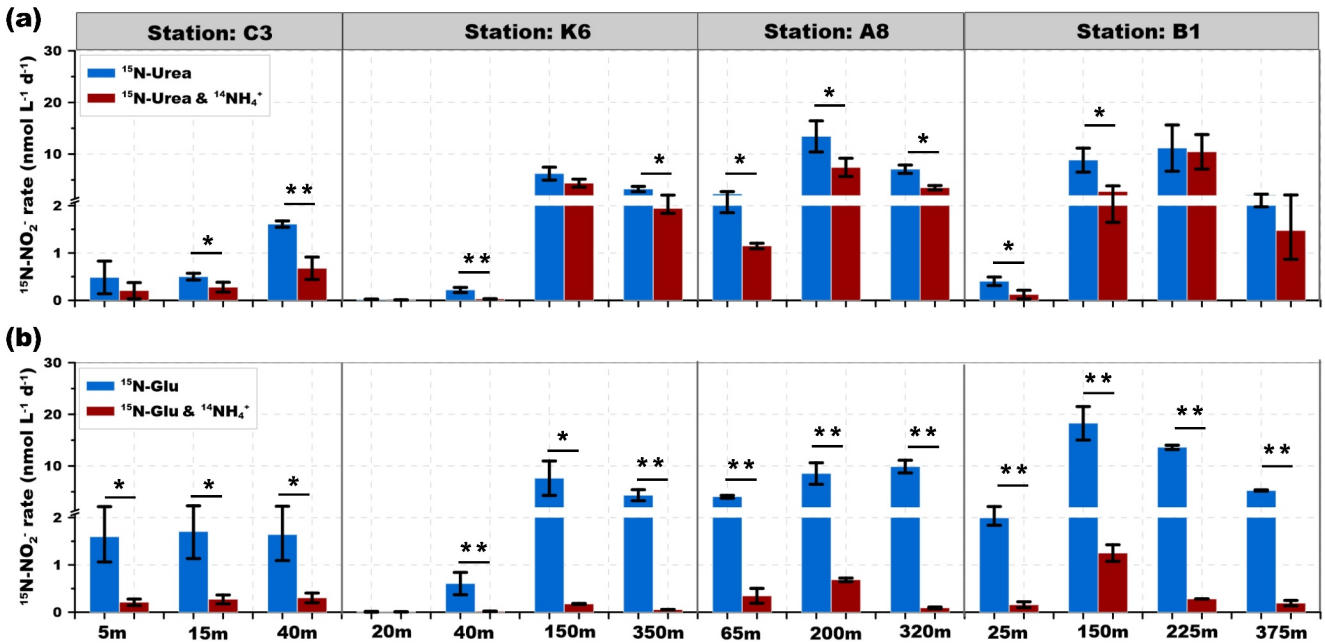

Figure 3. Comparison of urea and glutamic acid derived nitrogen oxidation from the 2015 NWP cruise. (a) $^{15}N\text{-}NO_2^-$ production rate in the ^{15}N-Urea labeling experiment. (b) $^{15}N\text{-}NO_2^-$ production rate in the ^{15}N-Glu labeling experiment. The blue bars and red bars depict the production rates without or with unlabeled NH_4^+ amendment, respectively. The error bars denote one standard deviation of triplicate rate measurements. (*) and (**) show the significance at 0.05 and 0.01 levels (*t* test), respectively.

decomposition of labile organics to NH_4^+ and its subsequent oxidation to NO_2^- are the main sources of NH_4^+ and NO_2^-, respectively (Santoro et al., 2019; W. Tang et al., 2023).

3.3. L-Glutamic Acid-Derived Nitrogen Oxidation Rate

^{15}N-Urea (100 nmol N L^{-1}) and ^{15}N-Glu (100 nmol N L^{-1}) derived nitrogen oxidation rates with or without the addition of unlabeled NH_4^+ (2,000 nmol N L^{-1}) were measured at four stations in the NWP. Without added NH_4^+, $^{15}N\text{-}NO_2^-$ production rate from both ^{15}N-Urea and ^{15}N-Glu followed similar spatial patterns across stations and depths. The rate was generally higher from ^{15}N-Glu (0.01–18.3, median 4.2 nmol N L^{-1} d^{-1}) than from ^{15}N-Urea (0.02–13.4, median 2.2 nmol N L^{-1} d^{-1}), even though the two groups of rates were not statistically significant ($p > 0.05$) (Figure 3). The addition of unlabeled NH_4^+ decreased the $^{15}N\text{-}NO_2^-$ production rate in both ^{15}N-Urea and ^{15}N-Glu incubations. The effect was greater for the ^{15}N-Glu treatment; 9 of 14 depths showed a significant difference in $^{15}N\text{-}NO_2^-$ production rate with and without unlabeled NH_4^+ amendment for ^{15}N-Urea (Figure 3a) compared to 13 of 14 depths for ^{15}N-Glu ($p < 0.05$) (Figure 3b). The decrease in $^{15}N\text{-}NO_2^-$ production rate with NH_4^+ addition for ^{15}N-Urea (6%–86%, median 51%) was significantly less than the decrease for ^{15}N-Glu (15%–99%, median 92%) ($p < 0.01$).

3.4. Kinetics of Ammonia, Urea and Nitrite Oxidation

The dependence of ammonia, urea, and nitrite oxidation rates on substrate concentration (in situ concentration plus tracer) was investigated by adding different amounts of tracers at selected stations in the NWP and the wNPSG (Figure 4). Notably, not all the depths showed the typical M-M kinetics in response to substrate enrichment, that is, for ammonia oxidation, only 4 of the total 15 depths in the NWP cruise and 6 of 12 depths in the wNPSG cruise could be fitted using the M-M equation. Similarly, 5 of 12 and 6 of 12 depths demonstrated M-M type kinetic responses for urea-N oxidation and nitrite oxidation, respectively, in the wNPSG cruise. Lack of kinetic response was often due to undetectable rates at all substrate levels in surface samples, but also occurred at depths in the lower euphotic and mesopelagic zones.

For the depths that showed M-M type responses, the V_{max} of ammonia oxidation varied over three orders of magnitude (ranging from <0.1 nmol L^{-1} d^{-1} in the surface layer of station K11 in the SCS to >100 nmol L^{-1} d^{-1}

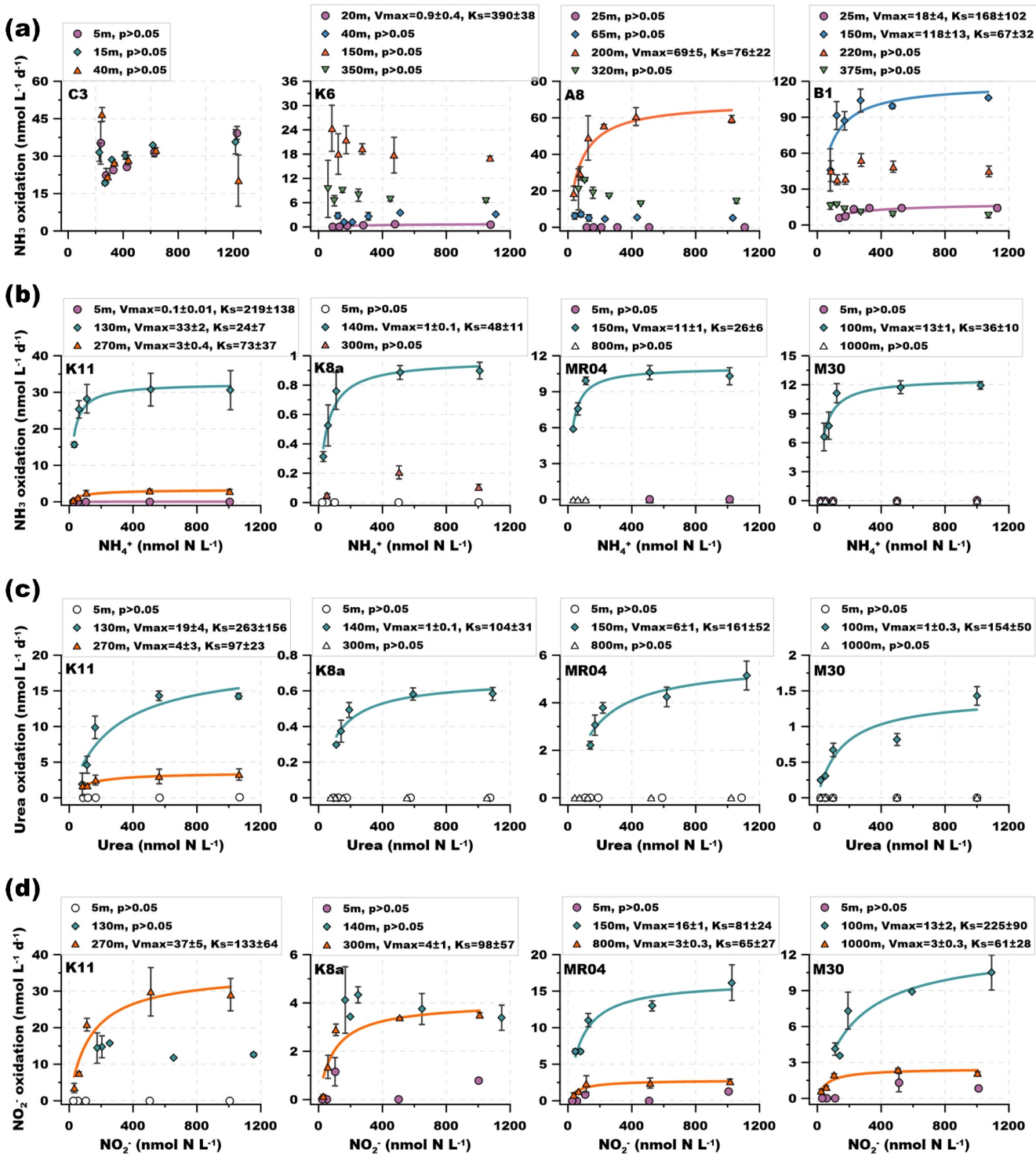

Figure 4. Kinetic behavior of ammonia, urea and nitrite oxidation. (a and b) The dependence of ammonia oxidation rate on total NH_4^+ concentration (in situ plus tracer concentration) in selected NWP 2015 cruise (C3, K6, K8, B1), SCS 2020 cruise (K11) and wNPSG 2021 cruise (K8a, MR04, M30) stations, respectively. (c and d) The dependence of urea and nitrite oxidation rate on total urea and NO_2^- concentration, respectively, in the SCS and wNPSG stations. The filled shapes indicate detectable rates, and the open shapes indicate rates below the detection limits. The error bars denote one standard deviation of triplicate rate measurements; in some cases, the error bars are smaller than the symbols. The solid lines represent the fitted M-M curves for depths that show significant relationship ($p < 0.05$) between substrate concentrations and rates.

at the base of the euphotic zone in the more productive B1 station in the NWP; Figures 4a and 4b). The differences in V_{max} and K_s between NWP and wNPSG were not statistically significant ($p > 0.05$), likely due to our limited number of observations. Vertically, the highest V_{max} values occurred in the vicinity of the PNM layer where the maximum in situ ammonia oxidation rates occurred. At this depth, the V_{max} and K_s values were highest in the NWP, followed by the SCS, and lowest in the wNPSG stations, suggesting the higher potential ammonia oxidation capacity and higher substrate requirement to reach V_{max} of the ammonia-oxidizing community in the more productive marine environment. This pattern suggests that both V_{max} and K_s of AOA natural populations are largely regulated by primary productivity as labile organic matter decomposition is the major source of NH_4^+ in the ocean (e.g., Gruber, 2008; Santoro et al., 2019; Ward & Zafiriou, 1988).

The kinetics of urea-N oxidation had a pattern similar to that of ammonia oxidation, with the highest V_{max} located in the vicinity of the PNM layer at the wNPSG stations (i.e., 100–140 m, Table S2 in Supporting Information S1). However, for those stations and depths where the kinetics of both ammonia oxidation and urea-N oxidation were determined, the measured V_{max} for urea-N oxidation (1–19 nmol N L^{-1} d^{-1}, median 3 nmol N L^{-1} d^{-1}) was lower than that for ammonia oxidation ($p < 0.01$), and the K_s value (97–263 nmol N L^{-1}, median 154 nmol N L^{-1}) was higher than that for ammonia oxidation ($p < 0.01$) (Figures 4b and 4c).

Unlike ammonia and urea-N oxidation, the highest V_{max} of nitrite oxidation was not consistently located at the PNM depth at the wNPSG stations (Figure 3; Table S2 in Supporting Information S1), and the depth with the highest in situ nitrite oxidation rate was not captured for kinetic analysis. Thus, a relationship between the magnitude of V_{max} and the depth distribution of nitrite oxidation cannot be discerned. The K_s value of nitrite oxidation ranged from 61 to 225 nmol L^{-1} (median 90 nmol L^{-1}), which was higher than the K_s value of ammonia oxidation ($p < 0.05$), but was comparable to the K_s value of urea-N oxidation at the corresponding depths ($p > 0.05$) (Figure 4d). These results suggested a higher capability of marine nitrifiers in scavenging NH_4^+ relative to urea and NO_2^-.

3.5. Distribution of Urea-N Oxidation and Ammonia Oxidation in the Ocean

Our data compilation showed that in the heavily human-perturbed estuarine and coastal waters, urea and NH_4^+ concentrations are significantly correlated ($R^2 = 0.6$; $p < 0.01$), although both concentrations vary widely. The correlation is probably due to the fact that both urea and NH_4^+ in these coastal waters are largely sourced from human activities such as fertilization and wastewater discharge (Sipler & Bronk, 2015). NH_4^+ concentration in the coastal water (ranged from 0.03 to 59 μmol L^{-1}, median 3.0 μmol L^{-1}) is significantly higher than urea concentration (ranged from 0.03 to 5.35 μmol N L^{-1}, median 1.3 μmol N L^{-1}) ($p < 0.01$, $n = 75$) (Figures 5a and 6a). By comparison, urea and NH_4^+ concentrations are significantly lower in the slope and open oceans than in the coastal zone ($p < 0.01$), while no significant difference was found between urea and NH_4^+ concentrations in the epipelagic or mesopelagic zone in our compiled data set (Figures 5b, 5c, and 6a). The urea to NH_4^+ ratio shows a stepwise increase; the ratio in the coastal water (median 0.3) is lower than that in the epipelagic zone (median 2.5) ($p < 0.01$) and the ratio in the epipelagic zone is lower than that in the mesopelagic ocean (median 5.3) ($p < 0.01$) (Figure 6b).

Both the urea and ammonia oxidation rates vary over four orders of magnitude in the coastal water (Figure 5d). Urea oxidation rate ranges from 0.1 to 296 (median 6.9) nmol N L^{-1} d^{-1}, and ammonia oxidation rate varies from 0.4 to 6,541 (median 314) nmol N L^{-1} d^{-1} (Figure 6c). For the open ocean system, urea oxidation and ammonia oxidation rates are significantly correlated in the epipelagic zone, with median values of 2.3 and 7.1 nmol N L^{-1} d^{-1}, respectively (Figures 5e and 6c). The two rates further decline to 0.5 and 0.3 nmol N L^{-1} d^{-1}, respectively, in the mesopelagic zone (Figures 5f and 6c). Similar to the concentration ratio distribution, the urea oxidation to ammonia oxidation rate ratio also shows a stepwise increase from the coastal water (0.0004–5.4, median 0.03) to the epipelagic zone (0.008–2.9, median 0.4), and to the mesopelagic ocean (0.004–7.0, median 1.2). The ratio in the coastal water is significantly lower than that in the epipelagic zone ($p < 0.05$) and ratio in the epipelagic zone is lower than that in the mesopelagic ocean ($p < 0.01$) (Figure 6d). Correspondingly, the contribution of urea-N oxidation to total NO_2^- production (defined as sum of urea-N and ammonia oxidation) ranges from 0.04% to 84.3% (median 3.01%) in the coastal zone, which increases to 0.8%–74.3% (median 27.1%) in the epipelagic zone, and the contribution ranges from 0.4% to 87.5% (median 54.9%) in the mesopelagic zone.

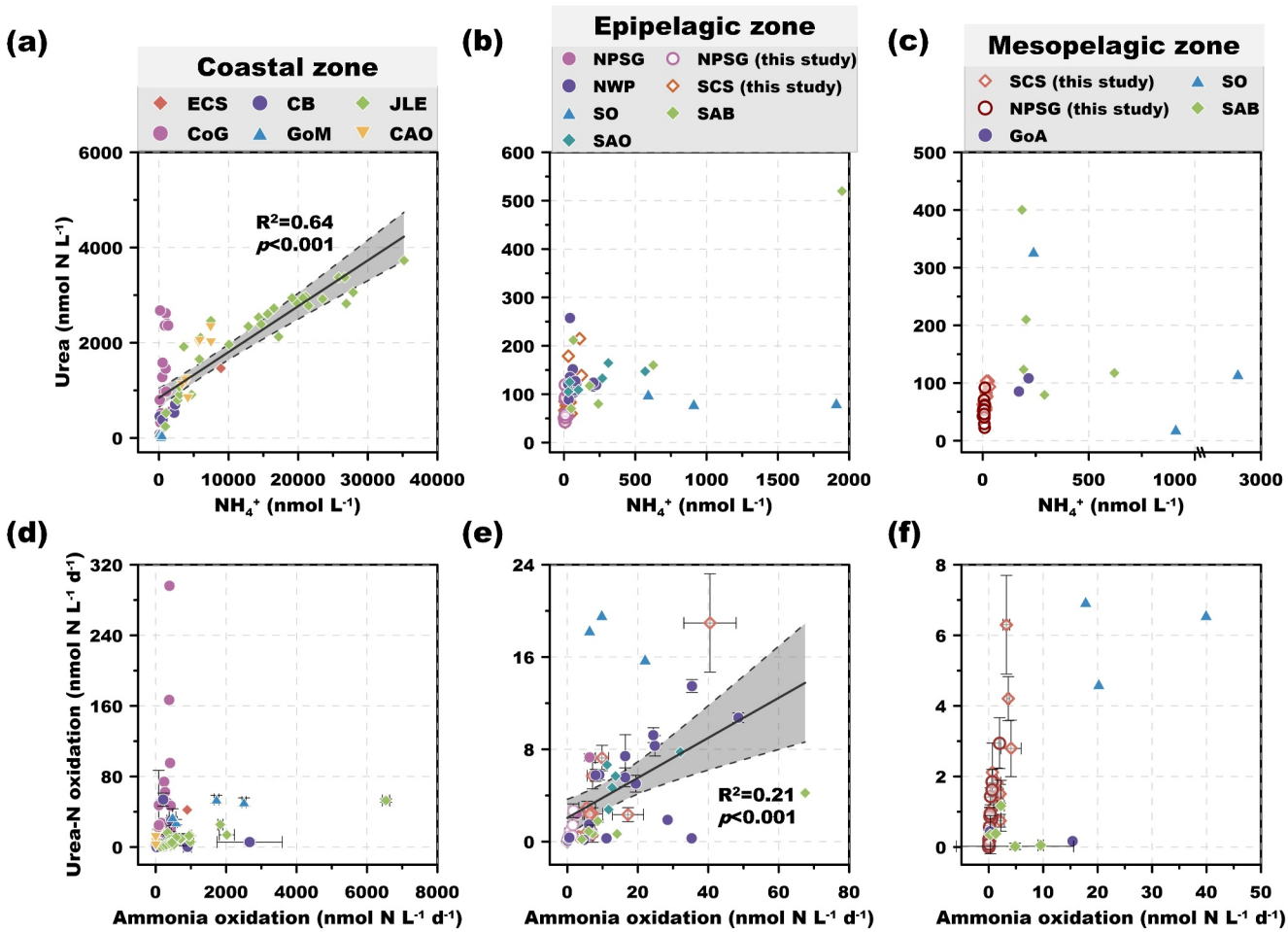

Figure 5. Compilation of urea and NH_4^+ concentrations and the oxidation rates measured in the global ocean. (a–c) Urea and NH_4^+ concentrations; (d–f) Urea and ammonia oxidation rates. The data set is divided into three groups: the coastal zone (a, d), the epipelagic zone (b, e), and the mesopelagic zone (c, f). Data sources for the coastal zone include the East China Sea (ECS) (Xu et al., 2019), the Gulf of Mexico (GoM) (Kitzinger et al., 2019), the Jiulong Estuary (JLE) (J. M. Tang et al., 2022), the coast of Georgia (CoG) (Damashek et al., 2019; Tolar et al., 2017), coast of the Arctic Ocean (CAO) (Shiozaki et al., 2021), and the Chesapeake Bay (CB) (W. Tang et al., 2022). Date source for the open ocean includes the North Pacific Subtropical Gyre (NPSG) and the Northwestern Pacific (NWP) (Wan et al., 2021; Xu et al., 2019), the Southern Ocean (SO); the South Atlantic Bight (SAB), the slope of Arctic Ocean (SAO) and the Gulf of Alaska (GoA) (Damashek et al., 2019; Shiozaki et al., 2021; Tolar et al., 2017), and rates measured in the South China Sea (SCS), NWP, and wNPSG from this study.

4. Discussion

4.1. Distinct Fate of Urea- and Glutamic Acid-Derived Nitrogen Implies Direct Oxidation of Urea to Nitrite

Although urea-N oxidation has been reported in various marine environments, whether the observed urea-N oxidation is performed by ammonia oxidizers or through the decomposition of urea by other microbes followed by ammonia oxidation, or both, is unclear, as different lines of evidence lead to different conclusions (e.g., Kitzinger et al., 2019; Santoro et al., 2017; Smith et al., 2016; Tolar et al., 2017). In our study, a significant fraction of ^{15}N-urea derived nitrogen was oxidized to $^{15}N\text{-}NO_2^-$ even in the presence of added $^{14}NH_4^+$, which reduced the measured $^{15}N\text{-}NO_2^-$ production rate by 6%–86% (median 51%) (Figure 3a). The ^{15}N-urea to $^{14}NH_4^+$ concentration ratio was less than 0.05 in the ^{15}N-urea plus $^{14}NH_4^+$ amendment experiment. By comparison, the ratio of ^{15}N-urea to $^{14}NH_4^+$ in the in situ water was >1 without $^{14}NH_4^+$ carrier amendment. Assuming the measured urea-N oxidation rate was sourced from urea decomposition by other microbes followed by ammonia oxidation (i.e., all by indirect urea-N oxidation pathway), we would expect to observe a 20-fold difference (95% reduction) of $^{15}N\text{-}NO_2^-$ production rate in the treatment with ^{15}N-urea plus $^{14}NH_4^+$ amendment compared to ^{15}N-urea only treatment. In contrast, our measured results showed a median of only 2-fold difference (51% reduction)

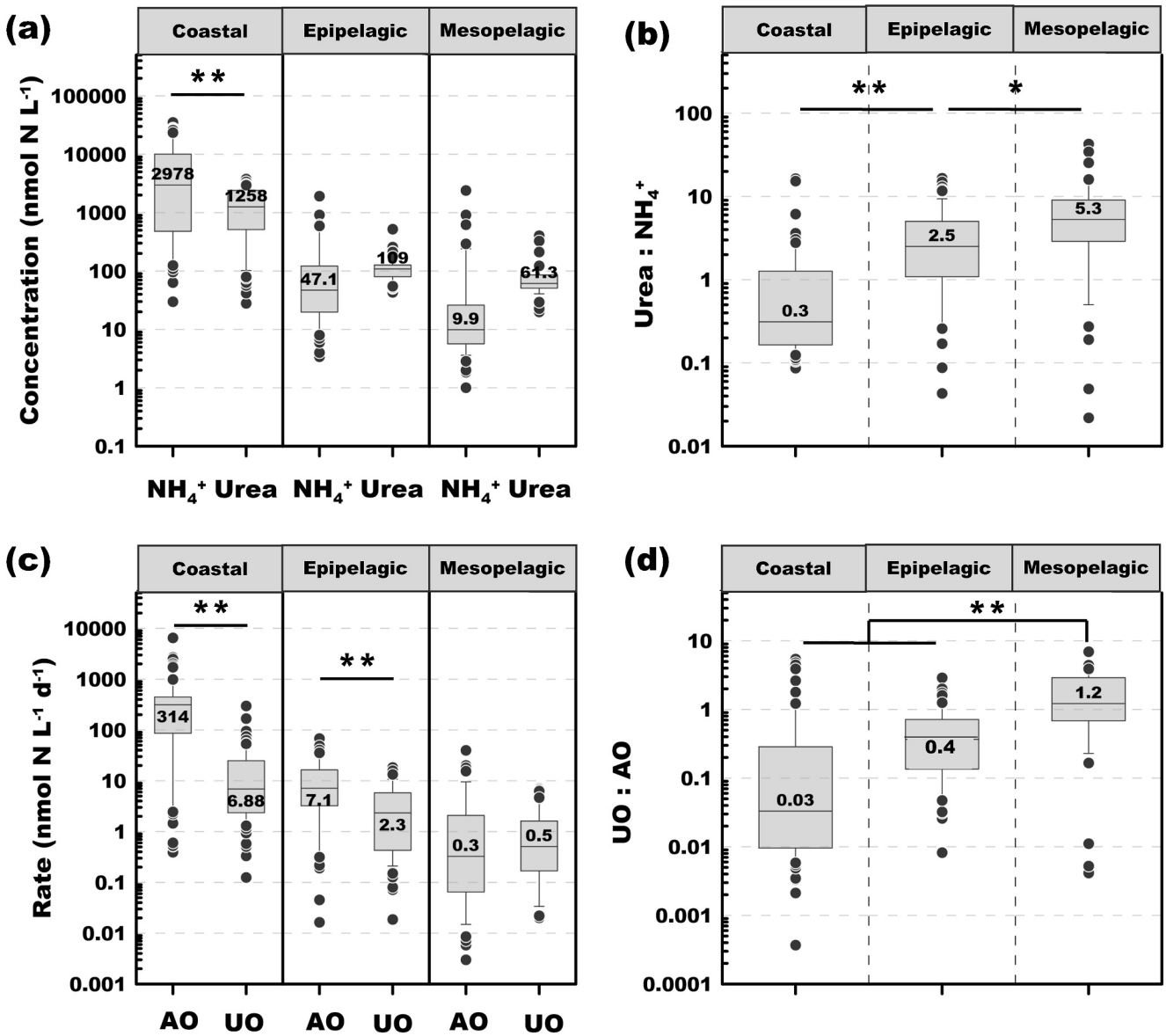

Figure 6. Box plots of urea and NH_4^+ concentrations and oxidation rates in the ocean. The data sources are shown in the caption of Figure 5. (a) NH_4^+ and urea concentration; (b) Statistics of NH_4^+ and urea concentration; (c) Ammonia and urea-N oxidation rate; (d) Statistics of ammonia and urea-N oxidation rate. AO and UO are the ammonia oxidation and urea-N oxidation rates. The numbers in the box plots show the median value, whiskers and boxes show the 10% and 90% percentile and 25%–75% quartile of the measurements, respectively. (*) and (**) show the significance at 0.05 and 0.01 levels, respectively.

between the two treatments. The results thus suggest that a large fraction of the measured $^{15}N\text{-}NO_2^-$ production rate in the ^{15}N-urea plus $^{14}NH_4^+$ treatment was due to direct urea-N oxidation. Alternatively, a direct linkage between urea degradation and ammonia oxidation in a microbial consortium with the NH_4^+ released by urea decomposition directly accessed by ammonia oxidizers without exchange with the ambient water, such as the reciprocal feeding of ammonia oxidizers and ureolytic NOB (Koch et al., 2015) or cyanate-degrading NOB (Palatinszky et al., 2015), may also lead to a lesser decrease than the predicted value. However, more experimental evidence is needed to test this hypothesis.

The ^{15}N-Glu derived NO_2^- production rate and ^{15}N-urea oxidation rate were comparable in the treatments without $^{14}NH_4^+$ amendment ($p > 0.05$). However, ^{15}N-Glu derived NO_2^- production rate decreased dramatically (median 92%) upon addition of $^{14}NH_4^+$ (Figure 3b). This is a nearly 12.5-fold difference due to $^{14}NH_4^+$ addition between urea and glutamate as a source of NO_2^-. This result was more consistent with the 95% decrease predicted

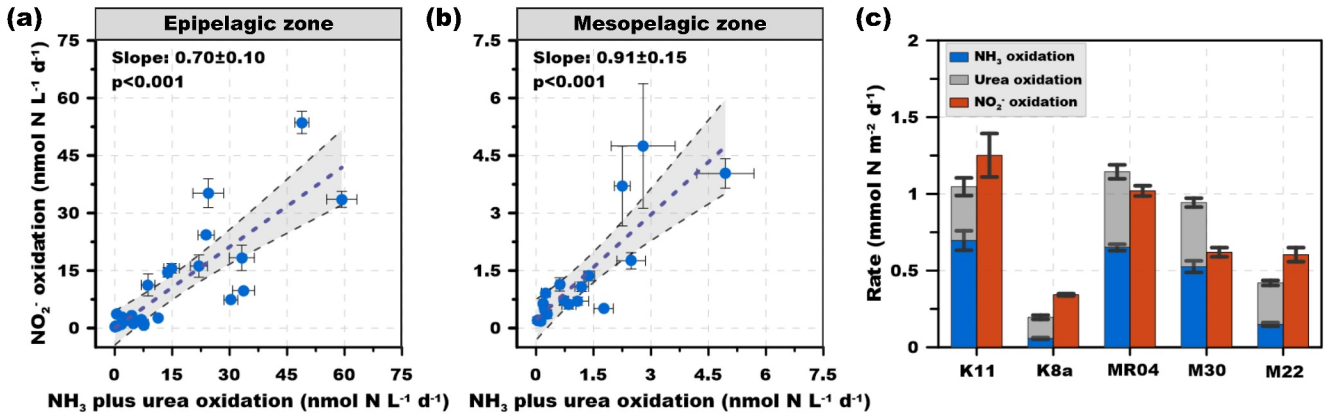

Figure 7. Comparison of NO_2^- production and consumption rates during nitrification. (a and b) Nitrite oxidation rate versus ammonia oxidation plus urea-N oxidation rate in the epipelagic zone and the mesopelagic zone, respectively. (c) Comparison of the depth-integrated (0–1,000 m) rates of ammonia oxidation, urea-N oxidation and nitrite oxidation. Note that the urea-N oxidation rate is added to the ammonia oxidation rate in panel (c). The error bars in panels (a) and (b) depict one standard deviation of triplicate rate measurements; in some cases, the error bars are smaller than the symbols. The black dashed line and gray shadow in panels (a) and (b) show linear regressions and the 95% confidence intervals, respectively. The error bars in panel (c) are the propagated standard deviation of the rates derived from triplicate incubations.

from the coupled heterotrophic decomposition-ammonia oxidation pathway. Although the in situ glutamate concentration was not measured in our study, previous measurements show an extremely low free glutamate concentration (<1 nmol L^{-1}) in the open ocean (Pèrez et al., 2003; Suttle et al., 1991), indicating a tight linkage between glutamate decomposition and ammonia oxidation or assimilation. The NH_4^+ sourced from glutamate decomposition thus apparently needs to be released to the ambient water before being accessed by the ammonia oxidizers, which was also observed in the South Atlantic Bight (Damashek et al., 2019). Combing the results of the distinctive response of ^{15}N-urea and ^{15}N-Glu derived nitrogen oxidation to $^{14}NH_4^+$ addition, we suggest that the observed $^{15}NO_2^-$ production in the ^{15}N-urea plus $^{14}NH_4^+$ addition treatment was largely sourced from direct urea-N oxidation. By comparison, the majority of ^{15}N-Glu supported ^{15}N-NO_2^- production was via coupled glutamate decomposition-ammonia oxidation. These results were consistent with the observation showing distinct fate and roles for different forms of labile DON in marine nitrification (Damashek et al., 2019).

4.2. Urea-N Oxidation Helps to Balance the Two Steps of Nitrification in the Oligotrophic Ocean

A recent compilation of ammonia oxidation and nitrite oxidation rate measurements in the global ocean shows decoupling of the two steps in nitrification, with the nitrite oxidation rate maxima generally located below the depth of the ammonia oxidation rate maxima and nitrite oxidation frequently exceeding the ammonia oxidation rate below the euphotic zone in the open ocean systems (W. Tang et al., 2023). Thus, not only are the rates vertically decoupled, but excess nitrite oxidation may indicate a missing of NO_2^- source in the dark ocean. Recent studies find that urea-derived nitrogen contributes ~20%–30% of NO_2^- production compared to ammonia oxidation, playing an additional role in NO_2^- production and PNM formation in the sunlit ocean (Laperriere et al., 2021; Wan et al., 2021). Our data showed that urea-N oxidation contributes to 36% of total NO_2^- production from urea-N and ammonia oxidation in the epipelagic zone, and the contribution increased to 45% in the mesopelagic zone of the SCS and wNPSG stations, indicating a substantial contribution of urea-N oxidation to NO_2^- production in the oligotrophic ocean.

To further quantify the role of urea-N oxidation in contributing to the balance of NO_2^- production and consumption during the nitrification process, we compared the rates of NO_2^- oxidation to total NO_2^- production from ammonia and urea-N oxidation in the SCS and the wNPSG stations where all three rates were measured simultaneously. Notably, given the different contribution of urea oxidation to NO_2^- production and the distinct AOA communities in the epipelagic and mesopelagic oceans, we compared NO_2^- production and consumption in these two layers separately (Figures 7a and 7b). The results showed that the nitrite oxidation rate was lower than the total NO_2^- production rate by ammonia oxidation plus urea-N oxidation (the ratio was 0.70 ± 0.10) in the epipelagic zone, indicating NO_2^- production by ammonia oxidizers was higher than NO_2^- consumption by nitrite oxidizers (Figure 7a), probably due to the higher light inhibition of nitrite oxidizers than ammonia oxidizers (Wan

et al., 2021). In the mesopelagic zone, the ratio increased to 0.91 ± 0.15, indicating nearly balanced NO_2^- production and consumption during the nitrification process (Figure 7b). The depth integrated urea-N oxidation rate was comparable to that of the ammonia oxidation rate, and the depth integrated nitrite oxidation rate was closer to the sum of urea-N oxidation and ammonia oxidation rates (Figure 7c). These results suggest that urea-N oxidation plays an important role in maintaining the balance of the two steps of nitrification in the oligotrophic ocean.

Although the potential utilization of other labile DON species, such as cyanate (Kitzinger et al., 2019; Palatinszky et al., 2015) and polyamine (Damashek et al., 2019), by marine ammonia oxidizers has also been reported in lab and field studies, the contribution of these compounds to NO_2^- production is probably limited in the oligotrophic ocean for the following reasons. First, cyanate and polyamine undergo rapid abiotic or biotic decomposition by heterotrophs in the ocean and therefore are usually present at trace levels (an order of magnitude lower than urea) (Kitzinger et al., 2019; Q. Liu et al., 2022; Lu et al., 2014; Widner et al., 2016). Second, the absence of known metabolic genes or pathways for cyanate and polyamine hydrolysis in marine ammonia oxidizers suggests that the metabolism of these organic N substrates may occur through alternative and potentially less efficient indirect processes (Damashek et al., 2019; Santoro et al., 2019), while many marine ammonia oxidizers possess urea transport and hydrolysis genes (Bayer et al., 2016; Qin et al., 2024). These lines of evidence suggest that urea-N oxidation might be primarily responsible for DON-derived NO_2^- production by marine ammonia oxidizers in the oligotrophic ocean.

4.3. Kinetic Traits Determine Marine NH_4^+, Urea and NO_2^- Distribution

We then explored the K_s of ammonia, urea, and nitrite oxidation in the marine environment because substrate affinity is considered a key trait in determining the capability of microbes to access and compete for substrates. Less than half of the depths (10 of the total 27 depths for ammonia oxidation, 5 of 12 depths for urea-N oxidation, and 6 of 12 depths for nitrite oxidation) investigated here demonstrated an M-M type response to substrate enrichment (Figure 4). The samples that did not show an M-M type response were grouped into three types: (a) The rate was below the detection limit at the low substrate end or the rate was too low to be detected at all tested substrate concentrations. These samples were mainly located at the surface layer (5 m) and the deeper mesopelagic zone (>800 m). Marine ammonia and nitrite oxidizers are known to be sensitive to light, and are outcompeted by phytoplankton at the surface of the oligotrophic ocean (Guerrero & Jones, 1996a, 1996b; Olson, 1981; Ward et al., 1982). Thus, the lack of detectable rate is likely due to the absence of nitrifiers or lack of nitrification activity in the surface water (Figure 2) (Santoro et al., 2019; W. Tang et al., 2023). For the deep water, both the abundance and activity of nitrifiers are restricted by substrate supply; this is particularly the case in the oligotrophic ocean where the organic flux is very low (Newell et al., 2013; Santoro et al., 2019). Although the geochemical data, for example, the accumulation of NO_3^- along with the consumption of dissolved oxygen, and the long residence time of NO_3^- in the deep water, provide evidence of the occurrence of nitrification in the ocean's interior, the activity of nitrifiers (and their low abundance) prohibits the detection of the oxidation rates in short-term incubations (Santoro et al., 2019; Ward & Zafiriou, 1988). (b) The rate was detectable but showed no response to substrate enrichment, typically observed at the depths with relatively high substrate concentration, such as ammonia oxidation at the coastal C3 station and the mid-latitude B1 station (NH_4^+ > 200 nmol L^{-1}), as well as nitrite oxidation at the PNM layer at K11 and K8a stations (NO_2^- > 140 nmol L^{-1}). The lack of rate enhancement by adding substrate could result from either substrate saturation or factors other than substrate concentrations, such as the trace metals iron and copper, in limiting the rate (Horak et al., 2013; Shiozaki et al., 2016; Ward, 2008). In our study, substrate saturation is probably the main cause of the lack of M-M type response in the coastal and more productive mid-latitude stations, while for the remote wNPSG stations, iron or copper limitation is more likely responsible for the absence of kinetic response, as our study area region is characterized by low iron and copper concentrations (König et al., 2021; Richon & Tagliabue, 2019). (c) We found a decrease in ammonia oxidation rate with ^{15}N-NH_4^+ enrichment at some depths at stations K6, A8, and B1 in our study. This unexpected apparent inhibition of ammonia oxidation by substrate was unlikely caused by ammonia toxicity as the highest NH_4^+ concentration in our experiment was ∼1 μmol L^{-1}, a level that is much lower than all known NH_4^+ inhibition concentrations for nitrifiers (L. Liu et al., 2021), even though a potential inhibition effect under such low NH_4^+ concentration cannot be fully excluded. A study conducted in the Southern Ocean finds a similar inhibition of ammonia oxidation rate by high $^{15}NH_4^+$ amendment (∼1 μmol L^{-1}) in waters with relatively high in situ NH_4^+ and is interpreted as a substrate saturation condition, but the potential cause for

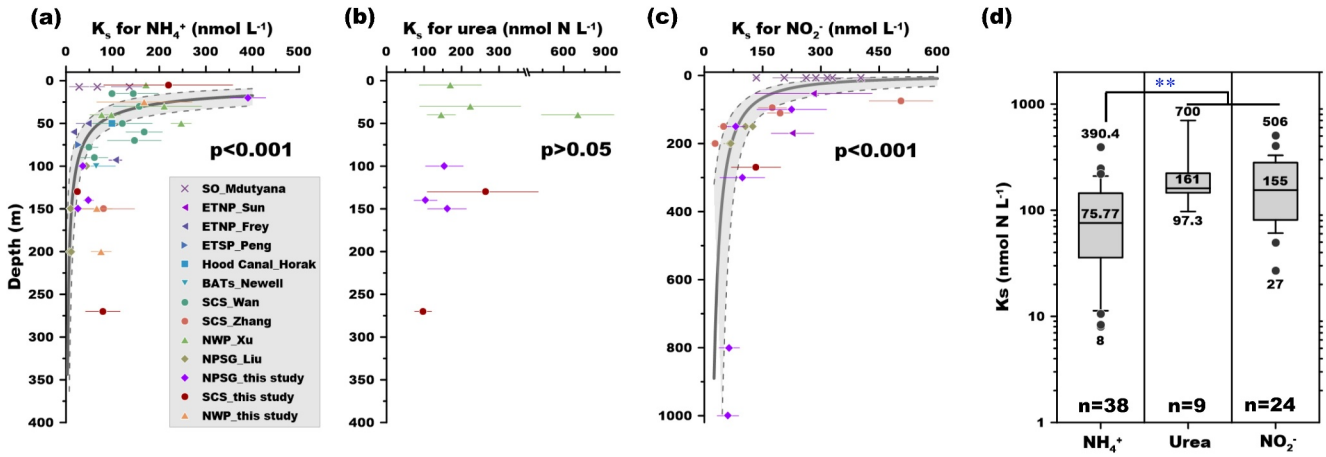

Figure 8. Vertical distribution and statistics of the K_s of ammonia, urea, and nitrite oxidation measured in the marine systems. (a–c) The compiled K_s for NH_4^+, urea, and NO_2^-, respectively. The solid lines represent the power law fitting curve (insignificant for K_s for urea). (d) Statistics of the K_s values. The numbers in the box plots show the minimum, median, and maximum values, whiskers and boxes show the 10% and 90% percentile and 25%–75% quartile of the measurements, respectively. The data sources are from the Sothern Ocean (SO) (Mdutyana, Marshall, et al., 2022; Mdutyana, Sun, et al., 2022), the Eastern Tropical North Pacific (ETNP) (Frey et al., 2022; Sun et al., 2017), Eastern Tropical South Pacific (ETSP) (Peng et al., 2016), the Hood Canal (Horak et al., 2013), BATS (Newell et al., 2013), the South China Sea (SCS) (Wan et al., 2018; Y. Zhang et al., 2020), the Northwestern Pacific (NWP) (Xu et al., 2019), the North Pacific Subtropical Gyre (NPSG) (L. Liu et al., 2023), and the results from this study. (**) shows the significance at 0.01 level.

the apparent inhibition is not discussed (Mdutyana, Sun, et al., 2022). Currently, we are unable to resolve the decrease of ammonia oxidation rate at NH_4^+ enrichment of ~1 μmol L^{-1}; future studies are warranted to examine the ubiquity and underlying reason for such an intriguing response.

For depths that exhibited typical M-M type kinetic response, the K_s of ammonia oxidation and nitrite oxidation varied between 24–390 nmol L^{-1} and 61–225 nmol L^{-1}, respectively, falling in the range of reported K_s in the open ocean systems (e.g., L. Liu et al., 2023; Mdutyana, Marshall, et al., 2022; Mdutyana, Sun, et al., 2022; Wan et al., 2018). For urea-N oxidation, the K_s varied in the range of 97–263 nmol N L^{-1}, which was higher than the K_s for NH_4^+ at the corresponding depths, suggesting a higher affinity toward NH_4^+ in marine AOA. This result is consistent with a recent pure culture-based investigation showing that the ureolytic marine AOA species possess higher affinity toward NH_4^+ than urea (Qin et al., 2024).

To investigate the spatial distribution of the K_s in the ocean, we added our results to a recently compiled data set (L. Liu et al., 2023). The results exhibited a power law profile of K_s for ammonia oxidation and nitrite oxidation as a function of water depth, although some data points measured in the mesopelagic zone of the SCS and the NWP stations were higher than the fitted values (Figures 8a and 8c). This increase in affinity for NH_4^+ and NO_2^- at greater depths suggests adaptation to the more limiting substrate levels at depth for AOA and NOB. By comparison, no significant vertical pattern was found for the K_s of urea-N oxidation, despite the fact that the highest K_s was observed in the upper euphotic zone (40 m) and the lowest K_s was observed in the mesopelagic zone (270 m) (Figure 8b). This lack of significant vertical trend might result from insufficient observations ($n = 9$), particularly the lack of observation in the mesopelagic zone (i.e., only one data point).

K_s values were elevated in the euphotic zone, where NH_4^+ and NO_2^- concentrations were relatively high although the K_s values varied among regions. The K_s value of ammonia oxidation was significantly lower than those of urea-N oxidation and nitrite oxidation (Figure 8c), demonstrating the higher capability of marine nitrifiers in scavenging NH_4^+ relative to urea and NO_2^-. For urea and nitrite oxidation, the K_s values were comparable in the euphotic zone. The K_s for NO_2^- decreased toward the greater depth to the minimum value of 27 nmol L^{-1}, while the lowest K_s value for urea remained at ~100 nmol N L^{-1}. These results suggest that the affinities of AOA and NOB in accessing their substrates might be important in controlling the distribution of NH_4^+, urea, and NO_2^- in the open ocean: in our study, high NH_4^+ concentrations were detected sporadically in the euphotic zone but at consistently low levels, that is, <10 nmol L^{-1} in the mesopelagic zone. NO_2^- concentration was also low except for the PNM at the base of the euphotic zone. By contrast, urea concentration was higher than NH_4^+ and NO_2^- concentrations throughout the water column except in the NH_4^+ maximum and PNM layers. Below the euphotic

zone, the low NH_4^+ and NO_2^- concentrations are maintained by the effective scavenging of NH_4^+ and NO_2^- by AOA and NOB in the dark ocean.

4.4. The Role of Urea-N Oxidation to NO_2^- Production Increases From Coastal to Oligotrophic Ocean

Since the first report of urea-N oxidation by marine AOA in the Arctic Ocean (Alonso-Sáez et al., 2012), urea-N oxidation has been investigated in several marine systems extending from coastal to open oceans, providing direct evidence for the contribution of urea in supporting energy metabolism for marine ammonia oxidizers. However, the relative magnitudes of urea-N oxidation and ammonia oxidation vary greatly among different regions, that is, the ratio of urea-N oxidation to ammonia oxidation ranges from less than 1% in the hyper-eutrophied Jiulong Estuary (J. M. Tang et al., 2022) to over 200% in the Arctic and Antarctic oceans (Shiozaki et al., 2021; Tolar et al., 2017). The cause of such high variability across different systems remains unexplained. A substantial subset of ammonia oxidizers possesses the genetic capability to utilize both ammonia and urea, and their substrate preference and regulation of urea and NH_4^+ utilization vary among major lineages (Qin et al., 2024). Thus, urea utilization may represent a key mechanism for niche partitioning and adaptation of ammonia oxidizers to different environmental settings.

The results of our data compilation suggest a geographic distribution pattern of urea-N oxidation and ammonia oxidation in the ocean (Figures 5 and 6). Both rates decrease from the coastal to the open ocean and the contribution of urea-N oxidation to NO_2^- production increases along the same gradient. The increasing ratio of urea-N oxidation to ammonia oxidation rate parallels the increase in the urea: NH_4^+ concentration ratio, indicating regulation of NH_4^+ and urea utilization strategy in marine ammonia oxidizers by the relative substrate concentration. These variations in urea and ammonia oxidation rates translate into variable contributions to NO_2^- production in the open ocean. The high urea-N oxidation to ammonia oxidation rate ratio in the mesopelagic ocean reveals an important role for urea-N oxidation in NO_2^- production in the ocean's interior that has been underappreciated. Depth-integrated (0–1,000 m) urea-N oxidation and ammonia oxidation rates were comparable in the SCS and the wNPSG (Table 1). If the same scale applies to the global ocean, NO_2^- production rates by ammonia oxidizers in the ocean might currently be underestimated substantially if NH_4^+ is considered the only substrate for marine AOA. We note, however, that the co-varying relationship between urea: NH_4^+ and urea-N oxidation: ammonia oxidation observed in the global ocean is more complex at the regional scale and does not follow a consistent trend. For example, high urea-N oxidation: ammonia oxidation rate has been reported in the polar ocean despite the low urea: NH_4^+ ratio being low (Damashek et al., 2019; Shiozaki et al., 2021; Tolar et al., 2017). Such a result suggests other factors than substrate ratio in regulating urea-N oxidation versus ammonia oxidation, and the regulation of substrate ratio on the rate ratio might be region-dependent. Future efforts should be devoted to quantifying the contribution of direct versus indirect urea-N oxidation, and more measurements of urea and ammonia oxidation across the ocean, particularly in the vast oligotrophic ocean and the remote polar oceans where urea-N oxidation seems to contribute a large source of NO_2^- compared to ammonia oxidation, are needed to better assess the NO_2^- production budget in the global ocean. Moreover, given that ammonia oxidizers play a key role in marine dark carbon fixation (Herndl & Reinthaler, 2013; Y. Zhang et al., 2020) and nitrous oxide production (Ji et al., 2018; Wan et al., 2023), our results also indicate a potential role of urea-N oxidation in the marine carbon cycle and greenhouse gas production that should be investigated in the future.

5. Conclusions

Our measurements of nitrogen nutrient distribution, ammonia, urea, and nitrite oxidation rates and their dependence on substrate concentration in environments extending from the eutrophic coastal water to the oligotrophic SCS and wNPSG provided several new insights into marine nitrification. In particular, we demonstrated that urea-N oxidation is an important process for balancing the two steps of nitrification, contributing even more NO_2^- than ammonia oxidation in the mesopelagic zone of the oligotrophic ocean, indicating the need to revisit the nitrification flux, and the associated dark carbon fixation, nitrous oxide production, and dissolved oxygen consumption in the ocean's interior.

We observed distinct patterns of kinetic responses to substrate enrichment. The K_s of ammonia oxidation and nitrite oxidation fall in the range of reported values and have a depth distribution that could be described by a power law, suggesting increased affinity in accessing the decreasing substrate concentrations in the energy-

starved dark ocean. No clear vertical pattern was detectable for the K_s values of urea-N oxidation, which were higher than the K_s of ammonia oxidation at the corresponding depths. The underlying reason for the higher K_s of urea-N oxidation may be related to the different mechanism in accessing NH_4^+ and urea and/or the impact of indirect urea-N oxidation that is associated with another process carried out by different organisms and governed by their own kinetic parameters. Nevertheless, the result supports the recent finding of the preferential use of NH_4^+ by marine AOA (Qin et al., 2024), and explains the higher standing stock of urea than NH_4^+ in the oligotrophic ocean. We also found that a considerable fraction of samples showed no response to substrate enrichment due to the absence of a viable nitrifying assemblage in surface waters, the in situ substrate concentration being saturated, or rate limitation by some factor other than substrate. Finally, a contrasting response of ^{15}N-Urea and ^{15}N-Glu oxidation to $^{14}NH_4^+$ amendment indicated that a large fraction of urea was directly oxidized by marine AOA. In contrast, nearly all glutamate-derived ammonia oxidation was driven by coupled heterotrophic decomposition and ammonia oxidation, suggesting distinctive fates of different DON compounds in sustaining NO_2^- production. These findings provide new information to improve models for understanding and predicting nitrogen biogeochemistry in the ocean.

Conflict of Interest

The authors declare no conflicts of interest relevant to this study.

Data Availability Statement

All data needed to evaluate the conclusions in the paper are deposited in the Zenodo database that can be accessed through https://doi.org/10.5281/zenodo.13739429 (Wan, 2024).

Acknowledgments

We greatly appreciate the help of W. Zhang and Q. Wu during the research cruise to the Northwestern Pacific; and B. Zou for collecting the samples during the South China Sea cruise. We also thank T. Huang for the on-board measurement of NH_4^+, Z. Yuan, Y. Wu for NO_3^- and NO_2^- measurements, L. Chen for urea measurements. We are grateful to the crew of the R/V *Dongfanghong II* and R/V *Tan Kah Kee* for the onboard assistance and providing the CTD data. This work was supported by the National Natural Science Foundation of China through Grants 41890802, 92058204, 41721005 and 41849905. XSW and BBW acknowledge funding from the Simons Foundation through award No. 675459 to BBW.

References

Alonso-Sáez, L., Waller, A. S., Mende, D. R., Bakker, K., Farnelid, H., Yager, P. L., et al. (2012). Role for urea in nitrification by polar marine Archaea. *Proceedings of the National Academy of Sciences of the United States of America*, *109*(44), 17989–17994. https://doi.org/10.1073/pnas.1201914109

Bayer, B., Vojvoda, J., Offre, P., Alves, R. J. E., Elisabeth, N. H., Garcia, J. A. L., et al. (2016). Physiological and genomic characterization of two novel marine thaumarchaeal strains indicates niche differentiation. *The ISME Journal*, *10*(5), 1051–1063. https://doi.org/10.1038/ismej.2015.200

Carini, P., Dupont, C. L., & Santoro, A. E. (2018). Patterns of thaumarchaeal gene expression in culture and diverse marine environments. *Environmental Microbiology*, *20*(6), 2112–2124. https://doi.org/10.1111/1462-2920.14107

Casciotti, K. L. (2016). Nitrite isotopes as tracers of marine N cycle processes. *Philosophical Transactions of the Royal Society A: Mathematical, Physical & Engineering Sciences*, *374*(2081), 20150295. https://doi.org/10.1098/rsta.2015.0295

Chen, L., Ma, J., Huang, Y., Dai, M., & Li, X. (2015). Optimization of a colorimetric method to determine trace urea in seawater. *Limnology and Oceanography: Methods*, *13*(6), 303–311. https://doi.org/10.1002/lom3.10026

Dai, M., Luo, Y. W., Achterberg, E. P., Browning, T. J., Cai, Y., Cao, Z., et al. (2023). Upper ocean biogeochemistry of oligotrophic subtropical gyres: From nutrient sources to carbon export. *Review of Geophysics*, *61*(3), e2022RG000800. https://doi.org/10.1029/2022RG000800

Damashek, J., Tolar, B. B., Liu, Q., Okotie-Oyekan, A. O., Wallsgrove, N. J., Popp, B. N., & Hollibaugh, J. T. (2019). Microbial oxidation of nitrogen supplied as selected organic nitrogen compounds in the South Atlantic Bight. *Limnology & Oceanography*, *64*(3), 982–995. https://doi.org/10.1002/lno.11089

Francis, C. A., Roberts, K. J., Beman, J. M., Santoro, A. E., & Oakley, B. B. (2005). Ubiquity and diversity of ammoniaoxidizing archaea in water columns and sediments of the ocean. *Proceedings of the National Academy of Sciences of the United States of America*, *102*(41), 14683–14688. https://doi.org/10.1073/pnas.0506625102

Frey, C., Sun, X., Szemberski, L., Casciotti, K. L., Garcia-Robledo, E., Jayakumar, A., et al. (2022). Kinetics of nitrous oxide production from ammonia oxidation in the Eastern Tropical North Pacific. *Limnology & Oceanography*, *68*(2), 424–438. https://doi.org/10.1002/lno.12283

Granger, J., & Sigman, D. M. (2009). Removal of nitrite with sulfamic acid for nitrate N and O isotope analysis with the denitrifier method. *Rapid Communications in Mass Spectrometry*, *23*, 3753–3762. https://doi.org/10.1002/rcm.4307

Gruber, N. (2008). The marine nitrogen cycle: Overview and challenges. In D. G. Capone, D. A. Bronk, M. R. Mulholland, & E. J. Carpenter (Eds.), *Nitrogen in the marine environment* (2, pp. 1–50). Elsevier.

Guerrero, M. A., & Jones, R. D. (1996a). Photoinhibition of marine nitrifying bacteria. I. Wavelength-dependent response. *Marine Ecology Progress Series*, *141*, 183–192. https://doi.org/10.3354/meps141183

Guerrero, M. A., & Jones, R. D. (1996b). Photoinhibition of marine nitrifying bacteria. II. Dark recovery after monochromatic or polychromatic irradiation. *Marine Ecology Progress Series*, *141*, 193–198. https://doi.org/10.3354/meps141193

Herndl, G. J., & Reinthaler, T. (2013). Microbial control of the dark end of the biological pump. *Nature Geoscience*, *6*(9), 718–724. https://doi.org/10.1038/ngeo1921

Horak, R. E. A., Qin, W., Schauer, A. J., Armbrust, E. V., Ingalls, A. E., Moffett, J. W., et al. (2013). Ammonia oxidation kinetics and temperature sensitivity of a natural marine community dominated by Archaea. *The ISME Journal*, *7*(10), 2023–2033. https://doi.org/10.1038/ismej.2013.75

Irwin, A. J., & Oliver, M. J. (2009). Are ocean deserts getting larger? *Geophysical Research Letters*, *36*(18), L18609. https://doi.org/10.1029/2009gl039883

Ji, Q., Buitenhuis, E., Suntharalingam, P., Sarmiento, J. L., & Ward, B. B. (2018). Global nitrous oxide production determined by oxygen sensitivity of nitrification and denitrification. *Global Biogeochemical Cycles*, *32*(12), 1790–1802. https://doi.org/10.1029/2018gb005887

Jung, M. Y., Sedlacek, C. J., Kits, K. D., Mueller, A. J., Rhee, S. K., Hink, L., et al. (2022). Ammonia-oxidizing archaea possess a wide range of cellular ammonia affinities. *The ISME Journal*, *16*(1), 272–283. https://doi.org/10.1038/s41396-021-01064-z

Karner, K. B., DeLong, E. F., & Karl, D. M. (2001). Archaeal dominance in the mesopelagic zone of the Pacific Ocean. *Nature*, *409*(6819), 507–510. https://doi.org/10.1038/35054051

Kitzinger, K., Padilla, C. C., Marchant, H. K., Hach, P. F., Herbold, C. W., Kidane, A. T., et al. (2019). Cyanate and urea are substrates for nitrification by Thaumarchaeota in the marine environment. *Nature Microbiology*, *4*(2), 234–243. https://doi.org/10.1038/s41564-018-0316-2

Koch, H., Lücker, S., Albertsen, M., Kitzinger, K., Herbold, C., Spieck, E., et al. (2015). Expanded metabolic versatility of ubiquitous nitrite-oxidizing bacteria from the genus *Nitrospira*. *Proceedings of the National Academy of Sciences of the United States of America*, *112*(36), 11371–11376. https://doi.org/10.1073/pnas.1506533112

König, D., Conway, T. M., Ellwood, M. J., Homoky, W. B., & Tagliabue, A. (2021). Constraints on the cycling of iron isotopes from a global ocean model. *Global Biogeochemical Cycles*, *35*(9), e2021GB006968. https://doi.org/10.1029/2021gb006968

Laperriere, S. M., Morando, M., Capone, D. G., Gunderson, T., Smith, J. M., & Santoro, A. E. (2021). Nitrification and nitrous oxide dynamics in the Southern California Bight. *Limnology & Oceanography*, *66*(4), 1099–1112. https://doi.org/10.1002/lno.11667

Liu, L., Chen, M., Wan, X. S., Du, C., Liu, Z., Hu, Z., et al. (2023). Reduced primary nitrite maximum by cyclonic eddies in the northwest Pacific subtropical gyre. *Science Advances*, *9*(33), eade2078. https://doi.org/10.1126/sciadv.ade2078

Liu, L., Liu, M., Jiang, Y., Lin, W., & Luo, J. (2021). Production and excretion of polyamines to tolerate high ammonia, a case study on soil ammonia-oxidizing archaeon "*Candidatus* Nitrosocosmicus agrestis". *mSystems*, *6*(1), e01003-20. https://doi.org/10.1128/mSystems.01003-20

Liu, Q., Nishibori, N., & Hollibaugh, J. T. (2022). Sources of polyamines in coastal waters and their links to phytoplankton. *Marine Chemistry*, *242*, 104121. https://doi.org/10.1016/j.marchem.2022.104121

Lu, X., Zou, L., Clevinger, C., Liu, Q., Hollibaugh, J. T., & Mou, X. (2014). Temporal dynamics and depth variations of dissolved free amino acids and polyamines in coastal seawater determined by high-performance liquid chromatography. *Marine Chemistry*, *163*, 36–44. https://doi.org/10.1016/j.marchem

Martens-Habbena, W., Berube, P. M., Urakawa, H., de la Torre, J. R., & Stahl, D. A. (2009). Ammonia oxidation kinetics determine niche separation of nitrifying Archaea and Bacteria. *Nature*, *461*(7266), 976–979. https://doi.org/10.1038/nature08465

Mcllvin, M. R., & Altabet, M. A. (2005). Chemical conversion of nitrate and nitrite to nitrous oxide for nitrogen and oxygen isotopic analysis in freshwater and seawater. *Analytical Chemistry*, *77*(17), 5589–5595. https://doi.org/10.1021/ac050528s

Mdutyana, M., Marshall, T., Sun, X., Burger, J. M., Thomalla, S. J., Ward, B. B., & Fawcett, S. E. (2022). Controls on nitrite oxidation in the upper Southern Ocean: Insights from winter kinetics experiments in the Indian sector. *Biogeosciences*, *19*(14), 3425–3444. https://doi.org/10.5194/bg-19-3425-2022

Mdutyana, M., Sun, X., Burger, J. M., Flynn, R. F., Smith, S., Horsten, N. R., et al. (2022). The kinetics of ammonium uptake and oxidation across the Southern Ocean. *Limnology & Oceanography*, *67*(4), 973–991. https://doi.org/10.1002/lno.12050

Newell, S. E., Fawcett, S. E., & Ward, B. B. (2013). Depth distribution of ammonia oxidation rates and ammonia-oxidizer community composition in the Sargasso Sea. *Limnology & Oceanography*, *58*(4), 1491–1500. https://doi.org/10.4319/lo.2013.58.4.1491

Olson, R. J. (1981). Differential photoinhibition of marine nitrifying bacteria: A possible mechanism for the formation of the primary nitrite maximum. *Journal of Marine Research*, *39*, 227–238.

Palatinszky, M., Herbold, C., Jehmlich, N., Pogoda, M., Han, P., von Bergen, M., et al. (2015). Cyanate as an energy source for nitrifiers. *Nature*, *524*(7563), 105–108. https://doi.org/10.1038/nature14856

Peng, X. F., Fuchsman, C. A., Jayakumar, A., Warner, M. J., Devol, A. H., & Ward, B. B. (2016). Revisiting nitrification in the Eastern Tropical South Pacific: A focus on controls. *Journal of Geophysical Research-Oceans*, *121*(3), 1667–1684. https://doi.org/10.1002/2015jc011455

Pèrez, M. T., Pausz, C., & Herndl, G. J. (2003). Major shift in bacterioplankton utilization of enantiomeric amino acids between surface waters and the ocean's interior. *Limnology & Oceanography*, *48*(2), 755–763. https://doi.org/10.4319/lo.2003.48.2.0755

Polovina, J. J., Howell, E. A., & Abecassis, M. (2008). Ocean's least productive waters are expanding. *Geophysical Research Letters*, *35*(3), L03618. https://doi.org/10.1029/2007gl031745

Qin, W., Wei, S. P., Zheng, Y., Choi, E., Li, X., Johnston, J., et al. (2024). Ammonia-oxidizing bacteria and archaea exhibit differential nitrogen source preferences. *Nature Microbiology*, *9*(2), 524–536. https://doi.org/10.1038/s41564-023-01593-7

Qin, W., Zheng, Y., Zhao, F., Wang, Y., Urakawa, H., Martens-Habbena, W., et al. (2020). Alternative strategies of nutrient acquisition and energy conservation map to the biogeography of marine ammonia-oxidizing archaea. *The ISME Journal*, *14*(10), 2595–2609. https://doi.org/10.1038/s41396-020-0710-7

Richon, C., & Tagliabue, A. (2019). Insights into the major processes driving the global distribution of copper in the ocean from a global model. *Global Biogeochemical Cycles*, *33*(12), 1594–1610. https://doi.org/10.1029/2019GB006280

Santoro, A. E., Richter, R. A., & Dupont, C. L. (2019). Planktonic marine archaea. *Annual Review of Marine Science*, *11*(1), 131–158. https://doi.org/10.1146/annurev-marine-121916-063141

Santoro, A. E., Saito, M. A., Goepfert, T. J., Lamborg, C. H., Dupont, C. L., & DiTullio, G. R. (2017). Thaumarchaeal ecotype distributions across the equatorial Pacific Ocean and their potential roles in nitrification and sinking flux attenuation. *Limnology & Oceanography*, *62*(5), 1984–2003. https://doi.org/10.1002/lno.10547

Shiozaki, T., Furuya, K., Kurotori, H., Kodama, T., Takeda, S., Endoh, T., et al. (2011). Imbalance between vertical nitrate flux and nitrate assimilation on a continental shelf: Implications of nitrification. *Journal of Geophysical Research*, *116*(C10), C10031. https://doi.org/10.1029/2010JC006934

Shiozaki, T., Hashihama, F., Endo, H., Ijichi, M., Takeda, N., Makabe, A., et al. (2021). Assimilation and oxidation of urea-derived nitrogen in the summer Arctic Ocean. *Limnology & Oceanography*, *66*(12), 4159–4170. https://doi.org/10.1002/lno.11950

Shiozaki, T., Ijichi, M., Isobe, K., Hashihama, F., Nakamura, K. I., Ehama, M., et al. (2016). Nitrification and its influence on biogeochemical cycles from the equatorial Pacific to the Arctic Ocean. *The ISME Journal*, *10*(9), 2184–2197. https://doi.org/10.1038/ismej.2016.18

Sipler, R. E., & Bronk, D. A. (2015). Dynamics of dissolved organic nitrogen. In D. A. Hansell, & C. A. Carlson (Eds.), *Biogeochemistry of marine dissolved organic matter* (2, pp. 127–232). Academic Press. https://doi.org/10.1016/B978-0-12-405940-5.00004-2

Smith, J. M., Damashek, J., Chavez, F. P., & Francis, C. A. (2016). Factors influencing nitrification rates and the abundance and transcriptional activity of ammonia-oxidizing microorganisms in the dark northeast Pacific Ocean. *Limnology & Oceanography*, *61*(2), 596–609. https://doi.org/10.1002/lno.10235

Sun, X., Ji, Q., Jayakumar, A., & Ward, B. B. (2017). Dependence of nitrite oxidation on nitrite and oxygen in low-oxygen seawater. *Geophysical Research Letters*, *44*(15), 7883–7891. https://doi.org/10.1002/2017GL074355

Suttle, C. A., Chan, A. M., & Fuhrman, J. A. (1991). Dissolved free amino acids in the Sargasso Sea: Uptake and respiration rates, turnover times, and concentrations. *Marine Ecology Progress Series*, *70*, 189–199. https://doi.org/10.3354/meps070189

Tang, J. M., Xu, M. N., Lin, Y., Chen, H., Jin, H., Han, L. L., et al. (2022). The biological transformation of ammonium and urea in a eutrophic estuarine system in Southern China. *Frontiers in Marine Science*, *9*, 1040554. https://doi.org/10.3389/fmars.2022.1040554

Tang, W., Tracey, J. C., Carroll, L., Wallace, E., Lee, J. A., Nathan, L., et al. (2022). Nitrous oxide production in the Chesapeake Bay. *Limnology & Oceanography*, *67*(9), 2101–2116. https://doi.org/10.1002/lno.12191

Tang, W., Ward, B. B., Beman, M., Bristow, L., Clark, D., Fawcett, S., et al. (2023). Database of nitrification and nitrifiers in the global ocean. *Earth System Science Data Discussions*. https://doi.org/10.5194/essd-2023-194

Tolar, B. B., Wallsgrove, N. J., Popp, B. N., & Hollibaugh, J. T. (2017). Oxidation of urea-derived nitrogen by thaumarchaeota-dominated marine nitrifying communities. *Environmental Microbiology*, *19*(12), 4838–4850. https://doi.org/10.1111/1462-2920.13457

Wan, X. S. (2024). Dataset_urea oxidation in the oligotrophic ocean [Dataset]. *Zenodo*. https://doi.org/10.5281/zenodo.13739429

Wan, X. S., Hou, L., Kao, S. J., Zhang, Y., Sheng, H. X., Shen, H., et al. (2023). Pathways of N_2O production by marine ammonia-oxidizing archaea determined from dual isotope labeling. *Proceedings of the National Academy of Sciences of the United States of America*, *120*(11), e2220697120. https://doi.org/10.1073/pnas.2220697120

Wan, X. S., Sheng, H. X., Dai, M., Church, M. J., Zou, W., Li, X., et al. (2021). Phytoplankton-nitrifier interactions control the geographic distribution of nitrite in the upper ocean. *Global Biogeochemical Cycles*, *35*(11), e2021GB007072. https://doi.org/10.1029/2021GB007072

Wan, X. S., Sheng, H. X., Dai, M., Zhang, Y., Shi, D., Trull, T. W., et al. (2018). Ambient nitrate switches the ammonium consumption pathway in the euphotic ocean. *Nature Communications*, *9*(1), 915. https://doi.org/10.1038/s41467-018-03363-0

Ward, B. B. (2008). Nitrification in marine systems. In D. G. Capone, D. A. Bronk, M. R. Mulholland, & E. J. Carpenter (Eds.), *Nitrogen in the marine environment* (2, pp. 199–261). Elsevier.

Ward, B. B., Olson, R. J., & Perry, M. J. (1982). Microbial nitrification rates in the primary nitrite maximum off southern California. *Deep-Sea Research*, *29*(2), 247–255. https://doi.org/10.1016/0198-0149(82)90112-1

Ward, B. B., & Zafiriou, O. C. (1988). Nitrification and nitric oxide in the oxygen minimum of the eastern tropical North Pacific. *Deep-Sea Research, Part A: Oceanographic Research Papers*, *35*(7), 1127–1142. https://doi.org/10.1016/0198-0149(88)90005-2

Weigand, M. A., Foriel, J., Barnett, B., Oleynik, S., & Sigman, D. M. (2016). Updates to instrumentation and protocols for isotopic analysis of nitrate by the denitrifier method. *Rapid Communications in Mass Spectrometry*, *30*(12), 1365–1383. https://doi.org/10.1002/rcm.7570

Widner, B., Fuchsman, C. A., Chang, B. X., Rocap, G., & Mulholland, M. R. (2018). Utilization of urea and cyanate in waters overlying and within the eastern tropical North Pacific oxygen deficient zone. *FEMS Microbiology Ecology*, *94*(10), FIY138. https://doi.org/10.1093/femsec/fiy138

Widner, B., Mulholland, M. R., & Mopper, K. (2016). Distribution, sources, and sinks of cyanate in the coastal North Atlantic Ocean. *Environmental Science and Technology Letters*, *3*(8), 297–302. https://doi.org/10.1021/acs.estlett.6b00165

Xu, M. N., Li, X., Shi, D., Zhang, Y., Dai, M., Huang, T., et al. (2019). Coupled effect of substrate and light on assimilation and oxidation of regenerated nitrogen in the euphotic ocean. *Limnology & Oceanography*, *64*(3), 1270–1283. https://doi.org/10.1002/lno.11114

Zakem, E. J., Al-Haj, A., Church, M. J., van Dijken, G. L., Dutkiewicz, S., Foster, S. Q., et al. (2018). Ecological control of nitrite in the upper ocean. *Nature Communications*, *9*(1), 1206. https://doi.org/10.1038/s41467-018-03553-w

Zhang, J. Z. (2000). Shipboard automated determination of trace concentrations of nitrite and nitrate in oligotrophic water by gas-segmented continuous flow analysis with a liquid waveguide capillary flow cell. *Deep Sea Research Part I: Oceanographic Research Papers*, *47*(6), 1157–1171. https://doi.org/10.1016/s0967-0637(99)00085-0

Zhang, Y., Qin, W., Hou, L., Zakem, E. J., Wan, X., Zhao, Z., et al. (2020). Nitrifier adaptation to low energy flux controls inventory of reduced nitrogen in the dark ocean. *Proceedings of the National Academy of Sciences of the United States ofAmerica*, *117*(9), 4823–4830. https://doi.org/10.1073/pnas.1912367117

Zhu, Y., Sun, J., Wang, Y., Li, S., Xu, T., Wei, Z., & Qu, T. (2019). Overview of the multi-layer circulation in the South China Sea. *Progress in Oceanography*, *175*, 171–182. https://doi.org/10.1016/j.pocean.2019.04.001

Zhu, Y., Yuan, D., Huang, Y., Ma, J., & Feng, S. (2013). A sensitive flow-batch system for on board determination of ultra-trace ammonium in seawater: Method development and shipboard application. *Analytica Chimica Acta*, *794*, 47–54. https://doi.org/10.1016/j.aca.2013.08.009